AN ANALYSIS OF THE DYNAMICS OF TOWING CABLES

Millard Sherwood Firebaug

AN ANALYSIS OF THE DYNAMICS OF TOWING CABLES

by

Millard Sherwood Firebaugh (LTCDR)

S.B., Massachusetts Institute of Technology
(1961)

S.M., Massachusetts Institute of Technology
(1966)

Nav.E., Massachusetts Institute of Technology
(1966)

Submitted in partial fulfillment of the requirements for the
Degree of Doctor of Science

at the

Massachusetts Institute of Technology
January, 1972

An Analysis of the Dynamics of Towing Cables

Millard Sherwood Firebaugh

Submitted to the Department of Ocean Engineering in January 14, 1972, in partial fulfillment of the requirements for the degree of Doctor of Science.

Abstract

The linearized dynamic and kinematic equations for the three-dimensional motions of a faired towing cable in a uniform flow are formulated with special attention to the hydrodynamic forces. Sinusoidal kinematic boundary conditions are applied to the cable at the tow point and simple dynamic boundary conditions are applied at the towed body. Analysis is done in the frequency domain. The resulting equations are solved numerically. The method is shown to be applicable over a range of practical cases. A computational difficulty involving the interaction of growing solutions with round-off error is identified. Demonstrably the difficulty may be put off by increasingly precise computation. The effect of important physical parameters of the problem on the motions transmitted from the tow point down the cable to the towed body are evaluated. Results are understood in terms of the natural frequencies of the oscillatory modes which combine to produce the cable dynamics. A design principle is established for minimizing towed body motions by partially decoupling the tow point from the towed body using moderately extensible cables.

Thesis Supervisor: J. Nicholas Newman
Title: Professor of Naval Architecture

ACKNOWLEDGEMENTS

I greatly appreciate the advice of my thesis supervisor, Professor J. Nicholas Newman and the efforts of the other members of my committee, Professors E. E. Covert, J. H. Milgram and J. T. Christian. Financial support for this work was provided by the Naval Research and Development Center, Carderock, Maryland, through the efforts of Mr. W. E. Smith, Head, Ship Dynamics Simulation Branch. Captain W. F. Searle, USN(ret) was influential in the selection of the topic and in advising me concerning my doctoral studies and deserves special thanks. The capable typing of Miss Sandra Vivolo was a considerable assist.

The value of the patience and understanding of my wife, Barbara, through this whole experience is inestimable.

TABLE OF CONTENTS

LIST OF FIGURES

LIST OF TABLES

LIST OF SYMBOLS

A	cross-section area of unloaded cable
A_B	cross-sectional area of towed body
a	non-dimensional body displacement defined on pg. 33
a_x, a_y, a_z	accelerations in the x, y and z directions
a_1, a_2	fairing, hydrodynamic loading function, sine series coefficients
b	fairing breadth in the loaded condition
$\tilde{b}$	effective fairing breadth in unloaded condition
b_1, b_2	fairing, hydrodynamic loading function, cosine series coefficients
C	non-dimensional body drag defined on pg. 39
C_D	fairing drag coefficient
C_T	drag coefficient of towed body
c	fairing chord length in the loaded condition
$\tilde{c}$	effective fairing chord length in unloaded condition
D	non-dimensional drag defined on pg. 33
D_1, D_2, D_3, D_4, D_5, D_6, D_7	non-dimensional drags defined on pg. 34
d	non-dimensional cable and fairing displacement per unit length defined on pg. 33
E	modulus of elasticity of the cable
f_{ex}	external force on fairing
f_o	amplitude of external force on fairing
f_n, f_t	normal and tangential cable loading functions
f_x, f_y, f_z	towed body disturbing forces
G	hydrodynamic function defined on pg. 95

g	acceleration due to gravity
H	hydrodynamic function defined on pg. 95
h	non-dimensional fairing mass per unit length defined on pg. 33
$h\dot{z}$	heave perturbation velocity in x_o, y_o, z_o coordinate system
I_y	mass moment of inertia of fairing per unit length about y axis
J_o, J_1	Bessel's functions of the first kind defined on pg. 98
k	non-dimensional towed body added mass defined on pg. 39
ℓ	length of the cable
M	non-dimensional towed body mass defined on pg. 39
M_B	mass of towed body
M_w, $M_{\dot{w}}$, M_x, M_q, $M_{\dot{q}}$	hydrodynamic moment derivatives per unit length for moments about y axis with respect to subscripted variable
m	mass per unit length of cable and fairing in loaded condition
$\tilde{m}$	mass per unit length of fairing and cable in unloaded condition
m	fairing mass per unit length in loaded condition
$\tilde{m}$	effective fairing mass per unit length in unloaded condition
N	non-dimensional steady tension defined on pg. 33
n	non-dimensional perturbation tension defined on pg. 33
$\bar{n}$	complex amplitude of n
$\bar{n}_R$, $\bar{n}_I$	real and imaginary parts of complex amplitude of n
n_m	magnitude of n

p, q, r	rotational velocities about the x, y and z axes respectively
s	Eulerian distance coordinate along the cable
$s\hat{u}$	surge perturbation velocity in x_o, y_o, z_o coordinate system
$s\hat{w}$	sway perturbation velocity in x_o, y_o, z_o coordinate system
T	tension in the cable
T^*	steady configuration tension in the cable
$\hat{T}$	perturbation tension in the cable
t	time
U_o	steady tow velocity
u, v, w	velocities in the x, y, and z directions pg. 14 to 32
u, v, w	non-dimensional perturbation velocities in x, y, and z directions pg. 33 to 115
u^*, v^*, w^*	steady configuration velocities in the x, y, and z directions
$\hat{u}, \hat{v}, \hat{w}$	perturbation velocities in the x, y, and z directions
$\bar{u}, \bar{v}, \bar{w}$	complex amplitudes of u, v, w pg. 33 to 115
$\bar{u}_R, \bar{u}_I, \bar{v}_R, \bar{v}_I, \bar{w}_R, \bar{w}_I$	real and imaginary parts of complex amplitudes of u, v, w
u_o, v_o, w_o	velocities in the x_o, y_o, z_o coordinate directions
u_{om}, v_{om}, w_{om}	magnitude of u_o, v_o, w_o
$\forall$	volume per unit length of fairing and cable in loaded condition
$\tilde{\forall}$	volume per unit length of fairing and cable in unloaded condition
$\forall_B$	volume of towed body
X, Y, Z	force components in the x,y, and z directions with superscripts indicating contributions from various effects

$X_{\dot{u}}$, $Z_{\dot{w}}$, $Z_{\dot{q}}$, $K_{\dot{p}}$, $M_{\dot{w}}$, $M_{\dot{q}}$, $N_{\dot{r}}$	hydrodynamic force and moment derivatives per unit length of cable fairing in the x and z directions and about the x, y, and z axes respectively
X, Y, Z	non-dimensional body disturbing forces defined on pg. 39 from pg. 39 to pg. 78
x, y, z	cable oriented Cartesian coordinate axes
x_o, y_o, z_o	locally vertical Cartesian coordinate axes
x_G	distance from y axis to center of gravity of fairing segment
$\tilde{x}_G$	effective distance from origin of cable coordinate system to center of gravity of fairing segment
x_p	distance from y axis to point through which resultant viscous drag force of fairing per unit length acts
Y_o, Y_1	Bessel's functions of the second kind defined on pg. 98
Z_c	composite z component of fairing gravitation and inertial forces combined with external force of cable on fairing
Z_w, $Z_{\dot{w}}$, Z_x, Z_q, $Z_{\dot{q}}$	hydrodynamic force derivatives per unit length for forces in z direction with respect to subscripted variable
$Z^{(v)}$	z component of viscous drag force per unit length
Z_c	z component of force on fairing from cable
z_o	amplitude of fairing motion in z direction pg. 79 to pg. 101
α	fairing rotation angle about the y axis pg. 79 to pg. 101
α_o	amplitude of fairing rotation angle pg. 79 to pg. 101
α, β, ε	non-dimensional surge, heave and sway velocities in the cable coordinate system pg. 35 to pg. 78
$\bar{\alpha}$, $\bar{\beta}$, $\bar{\varepsilon}$	complex amplitudes of α, β, ε pg. 35 to pg. 78

β	angle of inclination of inflow velocity vector pg. 88 to pg. 89
γ	non-dimensional modulus of elasticity of the cable defined on pg. 33
δ	non-dimensionalization factor defined on pg. 33
ζ	non-dimensional Lagrangian distance along the cable defined on pg. 33
η	non-dimensional lateral added mass defined on pg. 33
λ	reduced frequency defined on pg. 95
μ	non-dimensional transverse added mass defined on pg. 33
μ_B	added mass of towed body
ν	non-dimensional angular frequency of excitation
ξ	non-dimensional distance of fairing center of gravity from cable coordinate system origin defined on pg. 33
ρ	water density
σ	Lagrangian distance coordinate along the cable
τ	non-dimensional time defined on pg. 33
Φ	steady configuration trail angle in non-dimensional equations
Φ_c	critical trail angle
ϕ	trail angle pg. 14 to pg. 32
ϕ	perturbation trail angle pg. 33 to pg. 115
ϕ^*	steady configuration trail angle
$\hat{\phi}$	perturbation trail angle
$\bar{\phi}$	complex amplitude of ϕ pg. 33 to pg. 115
$\bar{\phi}_R$, $\bar{\phi}_I$	real and imaginary part of complex amplitude of ϕ
ψ	kite angle pg. 14 to pg. 32
ψ	perturbation kite angle pg. 33 to pg. 115

ψ^*	steady configuration kite angle
$\hat{\psi}$	perturbation kite angle
$\overline{\psi}$	complex amplitude of ψ
$\overline{\psi}_R$, $\overline{\psi}_I$	real and imaginary parts of complex amplitude of ψ
ω	excitation frequency in radians per sec.
ω_{Pt}	transverse pendulum natural frequency
$\omega_{P\ell}$	lateral pendulum natural frequency
ω_{Tt}	transverse vibrating string natural frequency
$\omega_{T\ell}$	lateral vibrating string natural frequency
ω_s	longitudinal stress vibrations natural frequency

Other symbols are used only locally and defined where used.

Chapter 1

INTRODUCTION

Background

A ship tows a body suspended at the end of a long cable. The cable is slender and curvatures are small so bending moments are negligible. The ship proceeds at velocity U_o in a seaway and bounces around a lot. As it moves along its motion is somehow transmitted to the towed body through the cable. The central question addressed by this thesis is, "what motions are transmitted to the towed body through the cable?" Real towed body systems now generally employ a fairing that is mostly free to rotate about the cable. So the cable is assumed to have a freely rotating fairing attached. Real cables stretch under load so the cable is assumed to be extensible.

In the absence of any excitation a steady towing situation exists, a problem solved by Pode (1951). The basis of the solution of the unsteady problem with an excitation present will be the assumption that the motion consists of small perturbations of the motion variables about their steady values leading to linear equations. These equations may be solved in the time domain with the method of characteristics or in the frequency domain assuming sinusoidal excitations of the tow point. Although both approaches have merit the frequency domain solutions are compatible with the existing body of knowledge concerning ship motions and with a formulation of the hydrodynamics of cable fairings derived

from thin wing theory. Knowledge of the ocean wave spectrum combined with response amplitude operators for a given tow ship can be converted to a spectrum of tow point velocities making an understanding of cable dynamics in the frequency domain appropriate. The frequency domain approach will be pursued here.

Before proceeding to the details of this paper it may be instructive to compare the problem posed to the classical problem of the motions of a vibrating string. A string is stretched between two points whose locations are fixed. The tension in the string is considered constant throughout its length. For certain conditions its rest position is a straight line between the end points. The string is considered to be inextensible. Its motions are described by the wave equation $\psi_{tt} = c^2\psi_{xx}$ where ψ is the displacement of the string from its rest position.

The problem posed in this thesis differs from the classical vibrating string problem in the following respects: the boundary conditions are more complicated than the simple kinematic conditions described above. One boundary of the tow cable is subject to a kinematic condition consisting of prescribed motions. The other boundary is subject to a dynamic condition consisting of prescribed forces, themselves functions of the kinematic variables at the boundary. The tension in the cable is not constant throughout. In fact the tension increases in some fashion from the body end to the towpoint end of the cable. The equilibrium condition of the cable is a non-linear

space curve. The cable is extensible, and finally it is operating subject to hydrodynamic and gravitational forces. The towing cable is a complicated combination of a vibrating string, a compound pendulum and a distributed mass-spring system all with significant viscous damping.

The solution of the cable problem will in various ways include the solutions to these classical problems. Of course, the coupling between the various problems is considerable and so the features of each are only outstanding in certain special cases. This thesis will formulate the problem in its complexity, apply the frequency domain analysis to plausible designs and bring the above notions to mind again while interpreting the results.

Antecedents

The problem of determining the cable configuration for a steady tow was comprehensively solved by Pode (1951). Both before and after Pode's solution investigators have studied hydrodynamic loading functions for cables. Their work is summerized by Casarella and Parsons (1970). In the same survey a number of investigations into the unsteady motions of cables are also summarized, of which the work of Whicker is very relevant to this thesis.

Whicker (1957) studied the dynamics of an unfaired, inextensible cable with drag but no added mass. He examined the transverse and longitudinal motions of the cable in a plane parallel to the towing direction. He presented two schemes for solution, one employing the method of characteristics and the other a linearized frequency domain approach. Neither solution scheme could be fully implemented without extensive computer aid so only simplified special cases were worked out. The special cases considered in this thesis in Appendix III where coincident with those of Whicker, verify his results.

Abkowitz (1965, 1967) considered the torsional and lateral vibrations of a towing cable with the fairing bound to the cable. His interest was in establishing cable parameters for which this system would be stable with respect to hydrodynamic flutter. Abkowitz showed that for some cable and fairing parameters in the range of practical interest stability was marginal and flutter could be expected. Primarily because of flutter and more general kiting instabilities most faired cable systems now employ fairings which are more or less rotationally unrestrained.

Schram and Reyle (1968) used the method of characteristics to analyze the transverse, longitudinal and lateral motions of an inextensible cable system with drag but no added mass. They developed transfer functions comparing the amplitude of surface excitations to the amplitude of towed vehicle motion. Their analysis was complicated by the assumption that the

cable was inextensible. Then a pair of equations in the first order system are parabolic instead of hyperbolic creating difficulties for the well-posedness of the initial value problem.

Huffman (1969) considered an extensible bare cable towed system undergoing transverse and longitudinal vibrations while being towed through air. He used the method of characteristics to describe cable configurations, variations in tension and towed body displacements from equilibrium for various combinations of cable parameters. His method was fully implemented numerically and since all the equations were hyperbolic, was well posed. As mentioned before however, these solutions in the time domain are not particularly compatible with the spectral analysis of ship motions. Of course, Huffman's interest was not in sea systems but in air towed systems so that this incompatibility was not a detriment to his selection of the method of characteristics as the proper approach to the problem solution.

Kerney (1971) used a small pertubation scheme to analyze the two-dimensional motions of an inextensible cable with added mass. Kerney's frequency domain analysis differs little from the method applied here or from the original proposal of Whicker. In implementing his solution numerically he encountered difficulties left unresolved.

The concern of the present study is an extensible cable, with a freely rotating fairing attached, towing a body and excited by transverse, longitudinal and lateral motions

emanating from the tow ship. The significance of the freely rotating fairing is that it greatly reduces drag on the cable. It can transmit no moment to the cable but it can transmit a side force the nature of which will be investigated. The results of the study concern the response of the cable and the towed body to sinusoidal excitations.

Chapter 2

FORMULATION

Coordinate Systems

A right-handed Cartesian coordinate system moves with the local position of the cable with its x_o axis along the direction of the mean tow velocity U_o. The y_o axis points opposite to the direction of gravitational attraction and the z_o axis points to starboard. Another right-handed Cartesian system unsubscripted is imbedded in the towing cable in such a way that were the tow ship stationary with the cable hanging straight below this x, y, z system would point in the same directions as the x_o, y_o, z_o system at all points along the cable. When the tow ship is moving with velocity U_o through the stationary ocean the cable streams behind and below the tow ship in a complicated space curve so that at each point along the cable the cable coordinate system will point in different directions from the x_o,y_o, z_o system. The relation between the x, y, z system and the x_o, y_o, z_o system is defined at each point of the cable by two angles, the trail angle ϕ and the kite angle ψ. The trail angle ϕ is the angle measured between the y axis of the cable system and the x_o axis of the ship system considering a rotation about the z axis. The kite angle ψ is then formed by a rotation about the x axis. The relationship between the two systems shown in figure 2.1 is given by the following transformation matrix which is formed by a procedure similar to that of Abkowitz (1969).

$$\begin{pmatrix} x \\ y \\ z \end{pmatrix} = \begin{pmatrix} \sin\phi & -\cos\phi & 0 \\ \cos\psi\ \cos\phi & \cos\psi\ \sin\phi & \sin\psi \\ -\sin\psi\ \cos\phi & -\sin\psi\ \sin\phi & \cos\psi \end{pmatrix} \begin{pmatrix} x_o \\ y_o \\ z_o \end{pmatrix} \qquad (2.1)$$

In the case of steady towing as shown by Pode (1951) there is no kiting but there is a trail angle ϕ. In the ensuing analysis perturbations about the steady values are to be used. The trail angle and kite angle are written as the sum of steady values and perturbation values which are small compared with the steady values, thus

$$\phi = \phi^* + \hat{\phi}$$

$$\psi = \psi^* + \hat{\psi} \text{ and furthermore } \psi^* = 0.$$

Under these circumstances the transformation matrix elements may be expanded in a Taylor Series giving for the zeroth and first order in the perturbation quantities

$$\begin{pmatrix} x \\ y \\ z \end{pmatrix} = \begin{pmatrix} \sin\phi^*+\cos\phi^*\hat{\phi} & -\cos\phi^*+\sin\phi^*\hat{\phi} & 0 \\ \cos\phi^*-\sin\phi^*\hat{\phi} & \sin\phi^*+\cos\phi^*\hat{\phi} & \hat{\psi} \\ -\hat{\psi}\ \cos\phi^* & -\hat{\psi}\ \sin\phi^* & 1 \end{pmatrix} \begin{pmatrix} x_o \\ y_o \\ z_o \end{pmatrix} \qquad (2.2)$$

Angular velocities to first order in perturbation quantities are $\partial\hat{\psi}/\partial t$ and $\partial\hat{\phi}/\partial t$. Accelerations in the x, y, and z directions are given by

$$a_x = \frac{\partial \hat{u}}{\partial t} - v^* \frac{\partial \hat{\phi}}{\partial t}$$

$$a_y = \frac{\partial \hat{v}}{\partial t} + u^* \frac{\partial \hat{\phi}}{\partial t} \qquad (2.3a\text{-}c)$$

$$a_z = \frac{\partial \hat{w}}{\partial t} + v^* \frac{\partial \hat{\psi}}{\partial t}$$

where u, v, and w are the velocities of the cable in the x, y, and z directions respectively. As before the velocities are the sum of steady values and perturbation values, and can be written as

$$u = u^* + \hat{u}$$

$$v = v^* + \hat{v}$$

$$w = w^* + \hat{w} \text{ but } w^* = 0 \text{ so } w = \hat{w}$$

Dynamic Equations

Consider a differential element of a faired towing cable such as shown in figure 2.2. The components of forces in each of the three directions of the cable coordinate system must be in equilibrium. For the unsteady case contributions

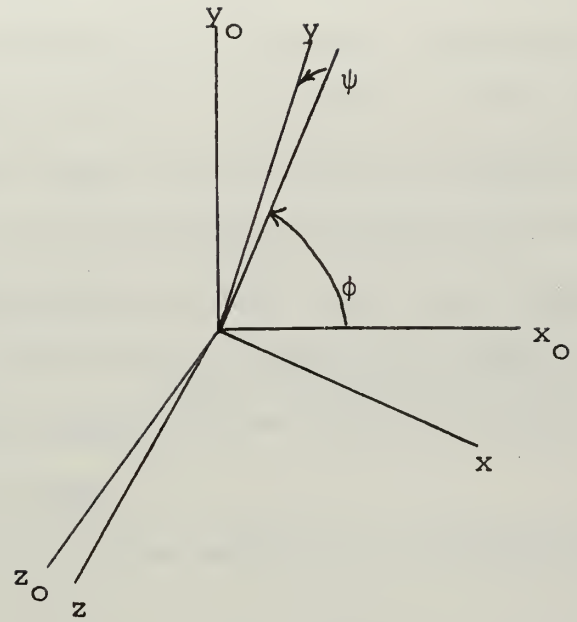

Figure 2.1

Coordinate Systems

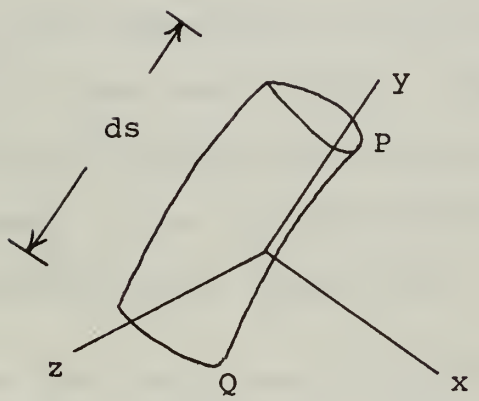

Figure 2.2

Differential Element of Faired Cable

to the forces are made by the inertia of the cable and the fairing, the tension in the cable, the weight of the cable and the fairing and the fluid flow over the surface of the fairing. Assume that the fairing is segmented into very short segments each of which is mounted on frictionless bearings on the cable so that forces are transmitted from the fairing to the cable but no twisting moment is transmitted. This assumption appears to be a fairly accurate description of many real systems.

The inertial forces acting on a differential element are

$$X^{(i)} = -mds\left(\frac{\partial \hat{u}}{\partial t} - v^* \frac{\partial \hat{\phi}}{\partial t}\right)$$

$$Y^{(i)} = -mds\left(\frac{\partial \hat{v}}{\partial t} + u^* \frac{\partial \hat{\phi}}{\partial t}\right) \qquad (2.4a\text{-}c)$$

$$Z^{(i)} = -mds\left(\frac{\partial \hat{w}}{\partial t} + v^* \frac{\partial \hat{\psi}}{\partial t}\right)$$

where the force components in the respective directions are given by the upper case letters. The mass per unit length of the cable and fairing is m and the length of the differential element in the loaded condition is ds.

The gravitational forces are:

$$X^{(g)} = (m-\rho\forall)ds\ g(\cos\phi^* - \sin\phi^*\hat{\phi})$$

$$Y^{(g)} = -(m-\rho\forall)ds\ g(\sin\phi^* + \cos\phi^*\hat{\phi}) \qquad (2.5a\text{-}c)$$

$$Z^{(g)} = (m-\rho\forall)ds\ g\hat{\psi}\sin\phi^*$$

where ρ is the density of the water in which the system is operating, $\forall$ is the volume per unit length of the fairing and cable in the loaded condition and g is the acceleration due to gravity.

The tension forces acting on the cable are

$$X^{(T)} = -T^* \frac{\partial \phi^*}{\partial s} ds - \hat{T} \frac{\partial \phi^*}{\partial s} ds - T^* \frac{\partial \hat{\phi}}{\partial s} ds$$

$$Y^{(T)} = \frac{\partial T^*}{\partial s} ds + \frac{\partial \hat{T}}{\partial s} ds \qquad (2.6a\text{-}c)$$

$$Z^{(T)} = T^* \frac{\partial \hat{\psi}}{\partial s} ds$$

where T is the tension which is the sum of a steady value and a perturbation value, that is $T = T^* + \hat{T}$.

The hydrodynamic forces acting on the cable may be written as

$$X^{(h)} = X^{*(h)} + \hat{X}^{(h)}$$

$$Y^{(h)} = Y^{*(h)} + \hat{Y}^{(h)} \qquad (2.7a\text{-}c)$$

$$Z^{(h)} = Z^{*(h)} + \hat{Z}^{(h)}$$

where as before, since the steady motion of the cable is in the x-y plane, $Z^{*(h)} = 0$. Appendix I contains the details of the hydrodynamic analysis and shows that the following equations may be written for (2.7a-c).

$$X^{(h)} = -C_D \tfrac{1}{2}\rho\, cds(a_1+a_2\sin\phi^*)\sin\phi^* U_o^2$$

$$-C_D \tfrac{1}{2}\rho\, cds[\{(a_1+a_2\sin\phi^*)2\sin^2\phi^*+(a_1+2a_2\sin\phi^*)$$

$$\cos^2\phi^*\}U_o\hat{u}+a_1\sin\phi^*\cos\phi^* U_o\hat{v}]-\tfrac{1}{4}\rho\pi b^2 ds\,\frac{\partial\hat{u}}{\partial t} \qquad (2.8a)$$

$$Y^{(h)} = -C_D \tfrac{1}{2}\rho\, cds(b_1+b_2\cos\phi^*)\cos\phi^* U_o^2$$

$$-C_D \tfrac{1}{2}\rho\, cds[b_1\sin\phi^*\cos\phi^* U_o\hat{u}+\{2(b_1+b_2\cos\phi^*)\cos^2\phi^*$$

$$+(b_1+2b_2\cos\phi^*)\sin^2\phi^*\}U_o\hat{v}]-\tfrac{1}{4}\rho\pi b^2 ds u^*\frac{\partial\hat{\phi}}{\partial t} \qquad (2.8b)$$

$$Z^{(h)} = -\tfrac{1}{2}\rho C_D\, cds(a_1+a_2\sin\phi^*)U_o\hat{w} - \tfrac{1}{4}\pi\rho c^2 ds\,\frac{\partial\hat{w}}{\partial t}$$

$$-4m\,\frac{x_G v^*}{c}\,ds\,\frac{\partial\hat{\psi}}{\partial t} \qquad (2.8c)$$

where b, c, m, x_G, C_D, a_1, a_2, b_1 and b_2 are defined in Appendix I. Equation (2.8c) is restricted to motions of the cable whose frequency corresponds to low reduced frequency, $\frac{\omega c}{U_o}$ and for fairings made of materials with densities close to that of sea water.

Combining equations (2.4a-c), (2.5a-c), (2.6a-c), and (2.8a-c) gives the dynamic equations for a differential element of cable.

$$-mds(\frac{\partial\hat{u}}{\partial t}-v^*\frac{\partial\hat{\phi}}{\partial t})+(m-\rho\forall)ds\; g(\cos\phi^*-\sin\phi^*\hat{\phi})-T^*\frac{\partial\phi^*}{\partial s}ds-\hat{T}\frac{\partial\phi^*}{\partial s}ds-T^*\frac{\partial\hat{\phi}}{\partial s}\,ds$$

$$-C_D\tfrac{1}{2}\rho cds(a_1+a_2\sin\phi^*)\sin\phi^* U_o^2-C_D\tfrac{1}{2}\rho cds[\{(a_1+a_2\sin\phi^*)2\sin^2\phi^*$$

$$+(a_1+2a_2\sin\phi^*)\cos^2\phi^*\}U_o\hat{u}+a_1\sin\phi^*\cos\phi^* U_o\hat{v}]-\tfrac{1}{4}\rho\pi b^2 ds\,\frac{\partial\hat{u}}{\partial t} = 0 \qquad (2.9a)$$

$$-mds\left(\frac{\partial\hat{v}}{\partial t}+u^*\frac{\partial\hat{\phi}}{\partial t}\right)-(m-\rho\forall)ds\ g(\sin\phi^*+\cos\phi^*\hat{\phi})+\frac{\partial T^*}{\partial s}ds+\frac{\partial\hat{T}}{\partial s}ds-\tfrac{1}{2}\rho C_D cds$$

$$(b_1+b_2\cos\phi^*)\cos\phi^* U_o^2-C_D\tfrac{1}{2}\rho cds[b_1\sin\phi^*\cos\phi^* U_o\hat{u}+\{2(b_1+b_2\cos\phi^*)$$

$$\cos^2\phi^*+(b_1+2b_2\cos\phi^*)\sin^2\phi^*\}U_o\hat{v}]-\tfrac{1}{4}\rho\pi b^2 ds u^*\frac{\partial\hat{\phi}}{\partial t}=0 \qquad (2.9b)$$

$$-mds\left(\frac{\partial\hat{w}}{\partial t}+v^*\frac{\partial\hat{\psi}}{\partial t}\right)+(m-\rho\forall)dsg\hat{\psi}\sin\phi^*+T^*\frac{\partial\hat{\psi}}{\partial s}ds-\tfrac{1}{4}\rho\pi c^2 ds\frac{\partial\hat{w}}{\partial t}-4m\frac{x_G}{c}v^*ds\ \frac{\partial\hat{\psi}}{\partial t}$$

$$-\tfrac{1}{2}\rho C_D cds(a_1+a_2\sin\phi^*)U_o\hat{w}=0 \qquad (2.9c)$$

Equations (2.9a,b) contain terms which are steady and terms which are first order in the time varying perturbation quantities. The steady terms may be separated from the time varying terms to yield a pair of equations describing the steady motion of the cable and a pair which pertain only to the time varying parts of the motion. The steady equations are

$$(m-\rho\forall)ds\ g\cos\phi^*-T^*\frac{\partial\phi^*}{\partial s}ds-\tfrac{1}{2}\rho C_D cds(a_1+a_2\sin\phi^*)\sin\phi^* U_o^2=0 \qquad (2.10a)$$

$$-(m-\rho\forall)ds\ g\sin\phi^*+\frac{\partial T^*}{\partial s}ds-\tfrac{1}{2}\rho C_D cds(b_1+b_2\cos\phi^*)\cos\phi^* U_o^2=0 \qquad (2.10b)$$

The time-varying equations are

$$-mds\left(\frac{\partial\hat{u}}{\partial t}-v^*\frac{\partial\hat{\phi}}{\partial t}\right)-(m-\rho\forall)ds\ g\sin\phi^*\hat{\phi}-\hat{T}\frac{\partial\phi^*}{\partial s}ds-T^*\frac{\partial\hat{\phi}}{\partial s}ds$$

$$-C_D\tfrac{1}{2}\rho cds[\{(a_1+a_2\sin\phi^*)2\sin^2\phi^*+(a_1+2a_2\sin\phi^*)\cos^2\phi^*\}U_o\hat{u}$$

$$+a_1\sin\phi^*\cos\phi^* U_o\hat{v}]-\tfrac{1}{4}\rho\pi b^2 ds\frac{\partial\hat{u}}{\partial t}=0 \qquad (2.11a)$$

$$-mds\left(\frac{\partial \hat{v}}{\partial t} + u^* \frac{\partial \hat{\phi}}{\partial t}\right) - (m-\rho V)ds\ g\ \cos\phi^* \hat{\phi} + \frac{\partial \hat{T}}{\partial s} ds - C_D \tfrac{1}{2} \rho c ds [b_1 \sin\phi^* \cos\phi^*$$

$$U_o \hat{u} + \{2(b_1 + b_2 \cos\phi^*)\cos^2\phi^* + (b_1 + 2b_2)\cos\phi^*)\sin^2\phi^*\} U_o \hat{v}]$$

$$-\tfrac{1}{4} \rho \pi b^2 ds\ u^* \frac{\partial \hat{\phi}}{\partial t} = 0 \qquad (2.11b)$$

Equations (2.10a,b) are the classical steady equations for a towed cable as determined by Pode (1951) and others. Equations (2.11a,b) and (2.9c) are the dynamic equations for the linearized three-dimensional motions of a faired cable.

Kinematic Equations

Kinematic relations for the differential element of cable must also be satisfied. Again consider the element shown in figure 2.2. Points P and Q can move relative to each other in three ways, one way along each of the intrinsic coordinate directions. Motion along the y direction comes from stretching the element. Motion in the x and z directions is caused by relative rotation of the element. The following relations express these relative motions. In the y direction

$$\frac{\partial v^*}{\partial s} ds + \frac{\partial \hat{v}}{\partial s} ds + u^* \frac{\partial \phi^*}{\partial s} ds + u^* \frac{\partial \hat{\phi}}{\partial s} ds + \hat{u} \frac{\partial \phi^*}{\partial s} ds = \frac{\partial}{\partial t} (ds) \qquad (2.12a)$$

In the x direction

$$\frac{\partial u^*}{\partial s} ds + \frac{\partial \hat{u}}{\partial s} ds - v^* \frac{\partial \phi^*}{\partial s} ds - \hat{v} \frac{\partial \phi^*}{\partial s} ds - v^* \frac{\partial \hat{\phi}}{\partial s} ds = - \frac{\partial \hat{\phi}}{\partial t} ds \qquad (2.12b)$$

and in the z direction

$$\frac{\partial \hat{w}}{\partial s} - u^* \hat{\psi} \frac{\partial \phi^*}{\partial s} ds + v^* \frac{\partial \hat{\psi}}{\partial s} ds = \frac{\partial \hat{\psi}}{\partial t} ds \tag{2.12c}$$

As in the case of the dynamic equations, the relations of equations (2.12a,b) contain steady terms and time-varying terms. The equations may then be separated each yielding two equations, one for the steady motion and one for the time-varying motion. Since there is no relative motion between points P and Q for the steady motion of the cable, the trivial results of the steady portion of equations (2.12a,b) is expected, namely that they are satisfied by $u^* = \sin\phi^*$ and $v^* = \cos\phi^*$. The time-varying portions give

$$\frac{\partial \hat{v}}{\partial s} ds + u^* \frac{\partial \hat{\phi}}{\partial s} ds + \hat{u} \frac{\partial \phi^*}{\partial s} ds = \frac{\partial}{\partial t} (ds) \tag{2.13a}$$

$$\frac{\partial \hat{u}}{\partial s} ds - \hat{v} \frac{\partial \phi^*}{\partial s} ds - v^* \frac{\partial \hat{\phi}}{\partial s} ds = - \frac{\partial \hat{\phi}}{\partial t} ds \tag{2.13b}$$

The dynamic equations and the kinematic equations for the time-varying three-dimensional motions of the cable are six equations in six unknowns, namely the three perturbation translational velocities $\hat{u}$, $\hat{v}$, $\hat{w}$, the two perturbation angular velocities $\hat{\phi}$ and $\hat{\psi}$ and the perturbation tension $\hat{T}$. The equations for the x and y motion are coupled together and decoupled from the side motions in the z direction. All the equations are written in the two independent variables s and t. The

equations have space varying coefficients in the variables u*, v*, ϕ* and T* a set of variables which trivially reduce to ϕ* and T*. These quantities may be determined from the solution of the steady equations (2.10 a,b). Before proceeding to methods of solution some additional operations may be performed on the cable equations to simplify the analysis.

Lagrangian Coordinate

Because the cable can stretch and because the amount of stretch is a function of the tension T, the independent variable s in the above equations, which measures length along the cable, is difficult to identify. To reach some specific value of s on the cable the observer must know the exact state of tension in the cable. A handier variable would be some distance between points fixed on the cable which was independent of the state of tension. Let us call this distance σ and measure it on the unstretched cable. This new variable is a Lagrangian coordinate in the sense that it is fixed to the particles of the cable. For extensible cables a simple relation exists between the Eulerian variable s and the Lagrangian variable σ; that is the stress-strain relation. If the stress-strain relation is linear then the relation between s and σ may be written as

$$\frac{\partial s}{\partial \sigma} = 1 + \frac{T}{AE} = 1 + \frac{T^*}{AE} + \frac{\hat{T}}{AE} \qquad (2.14)$$

where A is the cross-section area of the cable and E the modulus of elasticity. The Lagrangian coordinate σ may be introduced into the dynamic and kinematic equations by a change of variables from s to σ. There will also be a change in cable mass and volume per unit length and a change in cable dimensions as well as an effective change in fairing mass per unit length and fairing dimensions between the unstretched and stretched conditions of the cable. The relations are

$$m = \tilde{m}/\frac{\partial s}{\partial \sigma},\ c = \tilde{c}/\sqrt{\frac{\partial s}{\partial \sigma}},\ b = \tilde{b}/\sqrt{\frac{\partial s}{\partial \sigma}},\ \forall = \tilde{\forall}/\frac{\partial s}{\partial \sigma},\ \text{and}$$

$$x_G = \tilde{x}_G/\sqrt{\frac{\partial s}{\partial \sigma}},\ m = \tilde{m}/\frac{\partial s}{\partial \sigma} \qquad (2.15)$$

where the tilde indicates values for the unstretched cable. Making the variable change indicated by equation (2.14) and substituting in the relations of equations (2.15) gives for the steady configuration equations (2.10a,b)

$$(\tilde{m}-\rho\tilde{\forall})g\cos\phi^* - \tfrac{1}{2}\rho C_D\tilde{c}(a_1+a_2\sin\phi^*)\sin\phi^* U_o^2\left(1+\frac{T^*}{AE}\right)^{\frac{1}{2}} - T^*\frac{d\phi^*}{d\sigma} = 0 \qquad (2.16a)$$

$$-(\tilde{m}-\rho\tilde{\forall})g\sin\phi^* - \tfrac{1}{2}\rho C_D\tilde{c}(b_1+b_2\cos\phi^*)\cos\phi^* U_o^2\left(1+\frac{T^*}{AE}\right)^{\frac{1}{2}} + \frac{dT^*}{d\sigma} = 0 \qquad (2.16b)$$

for the dynamic time-varying equations (2.11a,b) and (2.9c)

$$-\tilde{m}\left(\frac{\partial \hat{u}}{\partial t} - v^*\frac{\partial \hat{\phi}}{\partial t}\right) - (\tilde{m}-\rho\tilde{\forall})g\,\sin\phi^*\hat{\phi} - \hat{T}\frac{\partial \phi^*}{\partial \sigma} - T^*\frac{\partial \hat{\phi}}{\partial \sigma} - \tfrac{1}{2}\rho C_D\tilde{c}$$

$$\left[\{(a_1+a_2\sin\phi^*)2\sin^2\phi^* + (a_1+2a_2\sin\phi^*)\cos^2\phi^*\}U_o\hat{u}\right.$$

$$\left.+a_1\sin\phi^*\cos\phi^*U_o\hat{v}\right]\left(1+\frac{T^*}{AE}\right)^{\frac{1}{2}} - \tfrac{1}{4}\rho\pi\tilde{b}^2\frac{\partial \hat{u}}{\partial t} - \tfrac{1}{2}\rho C_D\tilde{c}(a_1+a_2\sin\phi^*)$$

$$\sin\phi^*U_o^2\left(1+\frac{T^*}{AE}\right)^{-\frac{1}{2}}\frac{1}{2AE}\hat{T} = 0 \qquad (2.17a)$$

$$-\tilde{m}\left(\frac{\partial \hat{v}}{\partial t} + u^*\frac{\partial \hat{\phi}}{\partial t}\right) - (\tilde{m}-\rho\tilde{\forall})g\,\cos\phi^*\hat{\phi} + \frac{\partial \hat{T}}{\partial \sigma} - \tfrac{1}{2}\rho C_D\tilde{c}\left[b_1\sin\phi^*\cos\phi^*U_o\hat{u}\right.$$

$$\left.+\{2(b_1+b_2\cos\phi^*)\cos^2\phi^* + (b_1+2b_2\cos\phi^*)\sin^2\phi^*\}U_o\hat{v}\right]\left(1+\frac{T^*}{AE}\right)^{\frac{1}{2}}$$

$$-\tfrac{1}{4}\rho\pi\tilde{b}^2u^*\frac{\partial \hat{\phi}}{\partial t} - \tfrac{1}{2}\rho C_D\tilde{c}(b_1+b_2\cos\phi^*)\cos\phi^*U_o^2\left(1+\frac{T^*}{AE}\right)^{-\frac{1}{2}}\frac{\hat{T}}{2AE} = 0 \qquad (2.17b)$$

$$-\tilde{m}\left(\frac{\partial \hat{w}}{\partial t} + v^*\frac{\partial \hat{\Psi}}{\partial t}\right) + (\tilde{m}-\rho\tilde{\forall})g\hat{\Psi}\sin\phi^* + T^*\frac{\partial \hat{\Psi}}{\partial \sigma} - \tfrac{1}{4}\rho\pi\tilde{c}^2\frac{\partial \hat{w}}{\partial t} - 4\tilde{m}\frac{\tilde{x}_G}{\tilde{c}}v^*\frac{\partial \hat{\Psi}}{\partial t}$$

$$-\tfrac{1}{2}\rho C_D\tilde{c}(a_1+a_2\sin\phi^*)U_o\left(1+\frac{T^*}{AE}\right)^{\frac{1}{2}}\hat{w} = 0 \qquad (2.17c)$$

The last term in each of equations (2.17a) and (2.17b) came from the time-varying part of the tension in the substitution of $\tilde{c}$ for c in the steady equations. Continuing the variable change the kinematic equations (2.13a,b) and (2.12c) give

$$\frac{\partial \hat{v}}{\partial \sigma} + u^*\frac{\partial \hat{\phi}}{\partial \sigma} + \hat{u}\frac{\partial \phi^*}{\partial \sigma} = \frac{1}{AE}\frac{\partial \hat{T}}{\partial t} \qquad (2.18a)$$

$$\frac{\partial \hat{u}}{\partial \sigma} - \hat{v}\frac{\partial \phi^*}{\partial \sigma} - v^*\frac{\partial \hat{\phi}}{\partial \sigma} = -\frac{\partial \hat{\phi}}{\partial t}\left(1+\frac{T^*}{AE}\right) \qquad (2.18b)$$

$$\frac{\partial \hat{w}}{\partial \sigma} - u^*\hat{\Psi}\frac{\partial \phi^*}{\partial \sigma} + v^*\frac{\partial \hat{\Psi}}{\partial \sigma} = \frac{\partial \hat{\Psi}}{\partial t}\left(1+\frac{T^*}{AE}\right) \qquad (2.18c)$$

completing the transformation of the equations of motion from the Eulerian to the Lagrangian cable coordinate.

Non-dimensionalization

The following definitions are made to facilitate non-dimensionalization of the cable equations.

$\Phi = \phi^*$ $\quad w = \hat{w}/U_o$ $\quad \zeta = \sigma/\ell$ $\quad \eta = \frac{1}{4}\rho\pi\tilde{c}^2/\tilde{m}$

$\phi = \hat{\phi}$ $\quad \sin\Phi = u^*/U_o$ $\quad \tau = tg/U_o$ $\quad D = \frac{1}{2}\rho\, C_D\tilde{c}U_o^2/\tilde{m}g$

$\psi = \hat{\psi}$ $\quad \cos\Phi = v^*/U_o$ $\quad \delta = U_o^2/\ell g$ $\quad \xi = \tilde{x}_G/\tilde{c}$

$u = \hat{u}/U_o$ $\quad N = T^*/\tilde{m}g\ell$ $\quad d = \rho\tilde{\forall}/\tilde{m}$ $\quad h = \tilde{m}/\tilde{m}$

$v = \hat{v}/U_o$ $\quad n = \hat{T}/\tilde{m}g\ell$ $\quad \mu = \frac{1}{4}\rho\pi\tilde{b}^2/\tilde{m}$ $\quad \gamma = AE/\tilde{m}g\ell$

Substituting these definitions into the equations of the previous section gives for the steady configuration

$$(1-d)\cos\Phi - D(a_1+a_2\sin\Phi)\sin\Phi(1+\frac{N}{\gamma})^{\frac{1}{2}} = N\frac{d\Phi}{d\zeta} \qquad (2.19a)$$

$$(1-d)\sin\Phi + D(b_1+b_2\cos\Phi)\cos\Phi(1+\frac{N}{\gamma})^{\frac{1}{2}} = \frac{dN}{d\zeta} \qquad (2.19b)$$

for the time-varying dynamic equations

$$(1+\mu)\frac{\partial u}{\partial\tau} - \cos\Phi\frac{\partial\phi}{\partial\tau} + N\frac{\partial\phi}{\partial\zeta} + D[\{(a_1+a_2\sin\Phi)2\sin^2\Phi +$$

$$(a_1+2a_2\sin\Phi)\cos^2\Phi\}u + a_1\sin\Phi\cos\Phi v](1+\frac{N}{\gamma})^{\frac{1}{2}} + (1-d)\sin\Phi\phi +$$

$$[\frac{D}{2\gamma}(a_1+a_2\sin\Phi)\sin\Phi\,(1+\frac{N}{\gamma})^{-\frac{1}{2}} + \frac{d\Phi}{d\zeta}]n = 0 \qquad (2.20a)$$

$$\frac{\partial v}{\partial \tau} + (1+\mu)\sin\Phi\frac{\partial \phi}{\partial \tau} - \frac{\partial n}{\partial \zeta} + D\left(1+\frac{N}{\gamma}\right)^{\frac{1}{2}} [b_1 \sin\Phi\cos\Phi u +$$

$$\{2(b_1+b_2\cos\Phi)\cos^2\Phi + (b_1+2b_2\cos\Phi)\sin^2\Phi\}v] + (1-d)\cos\Phi\phi$$

$$+ \frac{D}{2\gamma}(b_1+b_2\cos\Phi)\cos\Phi\left(1+\frac{N}{\gamma}\right)^{-\frac{1}{2}} n = 0 \qquad (2.20b)$$

$$(1+\eta)\frac{\partial w}{\partial \tau} + (1+4h\xi)\cos\Phi\frac{\partial \psi}{\partial \tau} - N\frac{\partial \psi}{\partial \zeta} - (1-d)\sin\Phi\psi +$$

$$D(a_1+a_2\sin\Phi)\left(1+\frac{N}{\gamma}\right)^{\frac{1}{2}} w = 0 \qquad (2.20c)$$

and finally for the kinematic equations

$$\frac{\partial u}{\partial \zeta} - \cos\Phi\frac{\partial \phi}{\partial \zeta} + \frac{1}{\delta}\left(1+\frac{N}{\gamma}\right)\frac{\partial \phi}{\partial \tau} - \frac{d\Phi}{d\zeta} v = 0 \qquad (2.20d)$$

$$\frac{\partial v}{\partial \zeta} + \sin\Phi\frac{\partial \phi}{\partial \zeta} - \frac{1}{\gamma\delta}\frac{\partial n}{\partial \tau} + \frac{d\Phi}{d\zeta} u = 0 \qquad (2.20e)$$

$$\frac{\partial w}{\partial \zeta} + \cos\Phi\frac{\partial \psi}{\partial \zeta} - \frac{1}{\delta}\left(1+\frac{N}{\gamma}\right)\frac{\partial \psi}{\partial \tau} - \sin\Phi\frac{d\Phi}{d\zeta}\psi = 0 \qquad (2.20f)$$

In order to ease the algebraic load the following non-dimensional drag coefficients are defined and will be used in later manipulations.

$$D_1 = D[(a_1+a_2\sin\Phi)\,2\sin^2\Phi + (a_1+2a_2\sin\Phi)\cos^2\Phi]$$

$$D_2 = Da_1\sin\Phi\cos\Phi$$

$$D_3 = D(a_1+a_2\sin\Phi)\sin\Phi$$

$$D_4 = Db_1 \sin\Phi\cos\Phi$$

$$D_5 = D[2(b_1+b_2\cos\Phi)\cos^2\Phi+(b_1+2b_2\cos\Phi)\sin^2\Phi]$$

$$D_6 = D(b_1+b_2\cos\Phi)\cos\Phi$$

$$D_7 = D(a_1+a_2\sin\Phi)$$

Equations (2.19a,b) can be integrated to provide the information from which the coefficients of equations (2.20a-f) may be determined. Equations (2.20a-f) may be solved by techniques described later. Before we can proceed to a solution of these equations, conditions for the behavior of the system at the boundaries must be described.

Boundary Conditions

The six first order PDE's which comprise the model for the cable dynamics require six boundary conditions for their solution. Analysis in the characteristic plane shows that three conditions at each end of the cable need to be specified. Boundary conditions can be either dynamic or kinematic meaning that either the forces acting on or the motions of an end of the cable may be specified. Different combinations suit different problems. For example, a common towing situation involves a ship towing a cable and towed body which are small compared to the ship. Here there is little feedback from the cable dynamics to the ship motions so kinematic B.C.'s are

appropriate at the upper boundary of the cable. The motions of the towed body are not predictable in advance but the forces on the cables resulting from the motions of the towed body are, so dynamic conditions are appropriate at the lower boundary. Such a set of B.C.'s will be used for the remainder of this study. However, there are other interesting cases, notably the opposite of the above case which happens when a submerged submarine tows a surfaced buoy in which case the kinematic conditions are applied to the lower end of the cable and the dynamic conditions to the upper end. More complex B.C.'s will result for situations in which the towed body develops forces on the tow ship comparable to those resulting from its being in a seaway.

Specifying three dynamic B.C.'s amounts to specifying the three components of the force vector applied to the cable from the body in each of the three directions of the cable coordinate system. Similarly three kinematic conditions correspond to motions in each of the three directions. The simplest hydrodynamic shape which could be towed would be a sphere towed from its center of gravity. Such a shape would result in three simple equations which are developed in Appendix II. These equations for the dynamic boundary conditions at the towed body end of the cable are

$$-(M_B+\mu_B)\left(\frac{\partial \hat{u}}{\partial t} - v^*\frac{\partial \hat{\phi}}{\partial t}\right) - \tfrac{1}{2}\rho C_T A_B U_o^2 \left(\frac{u^*}{U_o} + \frac{\hat{u}}{U_o} + \frac{1}{U_o^3}\left(u^{*2}\hat{u}+u^*v^*\hat{v}\right)\right)$$

$$+(M_B-\rho\forall_B)g\cos\phi^* - (M_B-\rho\forall_B)g\sin\phi^*\hat{\phi} + f_x = 0 \qquad (2.21a)$$

$$-(M_B+\mu_B)\left(\frac{\partial \hat{v}}{\partial t} + u^*\frac{\partial \hat{\phi}}{\partial t}\right)-\tfrac{1}{2}\rho C_T A_B U_o^2\left(\frac{v^*}{U_o} + \frac{\hat{v}}{U_o} + \frac{1}{U_o^3}\ (v^{*2}\hat{v}+u^*v^*\hat{u})\right)$$

$$-(M_B-\rho\forall_B)g\ \sin\phi^*-(M_B-\rho\forall_B)g\ \cos\phi^*\hat{\phi}+T^*+\hat{T}+f_y = 0 \qquad (2.21b)$$

$$-(M_B+\mu_B)\left(\frac{\partial \hat{w}}{\partial t} +v^*\frac{\partial \hat{\psi}}{\partial t}\right) + (M_B-\rho\forall_B)g\ \hat{\psi}\ \sin\phi^* -\tfrac{1}{2}\rho C_T A_B U_o \hat{w}+f_z = 0 \qquad (2.21c)$$

where M_B is the mass of the body, $\forall_B$ its volume, μ_B its added mass, C_T its drag coefficient, A_B the cross sectional area of the body and f_x, f_y, f_z are disturbing forces applied to the body from the surroundings which will vanish for most circumstances.

The simplest conditions under which a body might be towed would be straight ahead on a calm sea. A slightly more complicated and more interesting condition is for the tow point to be moving ahead with velocity U_o but with superposed sinusoidal oscillations in velocity resulting from ship motions. Huffman (1969) considered a towed sphere and straight ahead motion of the tow point without oscillation. Unsteady motion was introduced by the disturbing forces on the sphere. Whicker (1957) considered the case for sinusoidal oscillations of the tow point. The former set of B.C.'s are particularly appropriate when using the method of characteristics to solve the cable dynamic equations. The latter approach is better for solution in the frequency domain. Once the frequency response of the tow system is known, the effect of a random excitation from the sea surface on the motions of the towed body may be evaluated.

Suppose the tow point is moving with the following velocities in the x_o, y_o, z_o coordinate system

$$u_o = U_o + s\hat{u}$$

$$v_o = h\hat{e}$$

$$w_o = s\hat{w}$$

where $s\hat{u}$, $h\hat{e}$, and $s\hat{w}$ are surge, heave, and sway perturbation velocities. These perturbation velocities are determined by resolution of the six degrees of freedom motions of the ship into translational velocities of the tow point. Application of the transformation (2.2) gives

$$u^* + \hat{u} = \sin\phi * U_o + \cos\phi * U_o\hat{\phi} + \sin\phi * s\hat{u} - \cos\phi * h\hat{e} \qquad (2.22a)$$

$$v^* + \hat{v} = \cos\phi * U_o - \sin\phi * U_o\hat{\phi} + \cos\phi * s\hat{u} + \sin\phi * h\hat{e} \qquad (2.22b)$$

$$\hat{w} = -\hat{\phi}\cos\phi * U_o + s\hat{w} \qquad (2.22c)$$

If the surface perturbations vanish, the result is Huffman's B.C.'s and if they are sinusoidal with frequency dependent amplitude, the result is Whicker's B.C.'s. Of course, the perturbations could be arbitrary functions of time if desired.

Equations (2.21) and (2.22) are a simple set of boundary conditions. More complicated dynamic conditions for the towed body are discussed in Appendix II. Equations (2.21) and (2.22) now need to be non-dimensionalized. The following definitions are made

$$M = M_B/\tilde{m}\ell,\quad k = \mu_B/\tilde{m}\ell,\quad C = \tfrac{1}{2}\rho C_T A_B u_o^2/\tilde{m}g\ell,\quad a = \rho\forall_B/\tilde{m}\ell$$

$$X = f_x/\tilde{m}g\ell,\quad Y = f_y/\tilde{m}g\ell,\quad Z = f_z/\tilde{m}g\ell$$

Applying the above definitions and separating the equations into steady and unsteady terms gives the steady B.C.'s at the towed body, that is for $\zeta = 0$

$$\Phi(0) = \tan^{-1}\left(\frac{M-a}{C}\right) \tag{2.23a}$$

$$N(0) = C\sqrt{1+\left(\frac{M-a}{C}\right)^2} \tag{2.23b}$$

and the time varying B.C.'s for $\zeta = 0$

$$-(M+k)\left(\frac{du}{d\tau} - \cos\Phi\frac{d\phi}{d\tau}\right) - C(u+\sin^2\Phi u+\sin\Phi\cos\Phi v) - (M-a)\sin\Phi\phi + X = 0 \tag{2.24a}$$

$$-(M+k)\left(\frac{dv}{d\tau} + \sin\Phi\frac{d\phi}{d\tau}\right) - C(v+\cos^2\Phi v+\sin\Phi\cos\Phi u) - (M-a)\cos\Phi\phi + n + Y = 0 \tag{2.24b}$$

$$-(M+k)\left(\frac{dw}{d\tau} + \cos\Phi\frac{d\psi}{d\tau}\right) - Cw + (M-a)\sin\Phi\phi + Z = 0 \tag{2.24c}$$

The steady kinematic B.C.'s at $\zeta = 1$ are trivially satisfied. The time varying conditions are

$$u = \cos\Phi\phi + \alpha \tag{2.25a}$$

$$v = -\sin\Phi\phi + \beta \tag{2.25b}$$

$$w = -\cos\Phi\psi + \varepsilon \tag{2.25c}$$

with $\alpha = (\sin\phi^* s\hat{u} - \cos\phi^* h\hat{e})/U_o$, $\beta = (\cos\phi^* s\hat{u} + \sin\phi^* h\hat{e})/U_o$, $\varepsilon = s\hat{w}/U_o$.

The problem is now formulated in sets of equations for the steady configuration, for the cable dynamics and kinematics and for the dynamic and kinematic boundary conditions.

Chapter 3

SOLUTION

Frequency Domain Analysis

Suppose the towed system is excited by sinusoidal oscillations of the tow point so that in equations (2.25a-c) we have for α, β, and ε

$$\alpha = \text{Re}\ \bar{\alpha}\ e^{i\nu\tau} \tag{3.1a}$$

$$\beta = \text{Re}\ \bar{\beta}\ e^{i\nu\tau} \tag{3.1b}$$

$$\varepsilon = \text{Re}\ \bar{\varepsilon}\ e^{i\nu\tau} \tag{3.1c}$$

where Re indicates that the real part is to be taken. This notation will hereafter be suppressed and it will be understood that the operation of taking the real part must be performed in interpreting results. Also $\tau = \frac{tg}{U_o}$ so $\nu = \frac{\omega U_o}{g}$ where ω is the usual angular frequency. Given the above excitation we assume solutions to equations (2.20a-f) of the form

$$u = \bar{u}(\zeta)e^{i\nu\tau} \text{ etc.} \tag{3.2}$$

These solutions are then substituted into equations (2.20a-f) resulting in a set of ordinary first order linear differential equations in the variables $\bar{u}(\zeta)$ etc. These equations cast into normal form are

$$\frac{d\bar{u}}{d\zeta} = \frac{\cos\Phi}{N}\left(-(1+\mu)i\nu\bar{u}+\cos\Phi i\nu\bar{\phi}-D_1(1+\frac{N}{\gamma})^{\frac{1}{2}}\bar{u}-D_2(1+\frac{N}{\gamma})^{\frac{1}{2}}\bar{v}-(1-d)\right.$$

$$\left.\sin\Phi\bar{\phi}-[\frac{D_3}{2\gamma}(1+\frac{N}{\gamma})^{-\frac{1}{2}}+\frac{d\Phi}{d\zeta}]\bar{n}\right)-\frac{1}{\delta}(1+\frac{N}{\gamma})i\nu\bar{\phi}+\frac{d\Phi}{d\zeta}\bar{v} \qquad (3.3a)$$

$$\frac{d\bar{v}}{d\zeta} = \frac{-\sin\Phi}{N}\left(-(1+\mu)i\nu\bar{u}+\cos\Phi i\nu\bar{\phi}-D_1(1+\frac{N}{\gamma})^{\frac{1}{2}}\bar{u}-D_2(1+\frac{N}{\gamma})^{\frac{1}{2}}\bar{v}-(1-d)\right.$$

$$\left.\sin\Phi\bar{\phi}-[\frac{D_3}{2\gamma}(1+\frac{N}{\gamma})^{-\frac{1}{2}}+\frac{d\Phi}{d\zeta}]\bar{n}\right)+\frac{1}{\gamma\delta}i\nu\bar{n}-\frac{d\Phi}{d\zeta}\bar{u} \qquad (3.3b)$$

$$\frac{d\bar{\phi}}{d\zeta} = \frac{1}{N}\left(-(1+\mu)i\nu\bar{u}+\cos\Phi i\nu\bar{\phi}-D_1(1+\frac{N}{\gamma})^{\frac{1}{2}}\bar{u}-D_2(1+\frac{N}{\gamma})^{\frac{1}{2}}\bar{v}-(1-d)\right.$$

$$\left.\sin\Phi\bar{\phi}-[\frac{D_3}{2\gamma}(1+\frac{N}{\gamma})^{-\frac{1}{2}}+\frac{d\Phi}{d\zeta}]\bar{n}\right) \qquad (3.3c)$$

$$\frac{d\bar{n}}{d\zeta} = i\nu\bar{v}+(1+\mu)\sin\Phi i\nu\bar{\phi}+D_4(1+\frac{N}{\gamma})^{\frac{1}{2}}\bar{u}+D_5(1+\frac{N}{\gamma})^{\frac{1}{2}}\bar{v}+(1-d)$$

$$\cos\Phi\bar{\phi}+\frac{D_6}{2\gamma}(1+\frac{N}{\gamma})^{-\frac{1}{2}}\bar{n} \qquad (3.3d)$$

$$\frac{d\bar{w}}{d\zeta} = \frac{-\cos\Phi}{N}\left((1+\eta)i\nu\bar{w}+(1+4h\xi)\cos\Phi i\nu\bar{\psi}-(1-d)\sin\Phi\bar{\psi}+D_7(1+\frac{N}{\gamma})^{\frac{1}{2}}\bar{w}\right.$$

$$\left.+\frac{1}{\delta}(1+\frac{N}{\gamma})i\nu\bar{\psi}+\sin\Phi\frac{d\Phi}{d\zeta}\bar{\psi}\right) \qquad (3.3e)$$

$$\frac{d\bar{\psi}}{d\zeta} = \frac{1}{N}\left((1+\eta)i\nu\bar{w}+(1+4h\xi)\cos\Phi i\nu\bar{\psi}-(1-d)\sin\Phi\bar{\phi}+D_7(1+\frac{N}{\gamma})^{\frac{1}{2}}\bar{w}\right) \qquad (3.3f)$$

Equations (3.3a-f) consist of real and imaginary parts. They may be further simplified by dividing the solutions into real and imaginary parts. That is

$$\bar{u} = \bar{u}_R + i\bar{u}_I \text{ etc.}$$

The above relations may be substituted into equations (3.3a-f) giving a set of twelve equations in the real and imaginary parts of the original six dependent variables. The boundary conditions may be similarly treated. The set of twelve equations with associated boundary conditions divide into two sets of coupled equations, one set of eight for the longitudinal-transverse vibrations and one set of four for the lateral vibrations. These two sets may be written in matrix form with their associated B.C.'s as shown below.

$$
\begin{pmatrix} \frac{d\bar{u}_R}{d\zeta} \\ \frac{d\bar{u}_I}{d\zeta} \\ \frac{d\bar{v}_R}{d\zeta} \\ \frac{d\bar{v}_I}{d\zeta} \\ \frac{d\bar{\phi}_R}{d\zeta} \\ \frac{d\bar{\phi}_I}{d\zeta} \\ \frac{d\bar{n}_R}{d\zeta} \\ \frac{d\bar{n}_I}{d\zeta} \end{pmatrix} =
\begin{pmatrix}
-\frac{\cos\Phi}{N} D_1 (1+\frac{N}{\gamma})^{\frac{1}{2}} & \frac{\cos\Phi}{N}(1+\mu)\nu & -[\frac{\cos\Phi}{N} D_2 (1+\frac{N}{\gamma})^{\frac{1}{2}} - \frac{d\Phi}{d\zeta}] & 0 & -\frac{\cos\Phi(1-d)\sin\Phi}{N} & -[\frac{\cos^2\Phi}{N} - \frac{1}{\delta}(1+\frac{N}{\gamma})]\nu & -\frac{\cos\Phi}{N}[\frac{D_3}{2\gamma}(1+\frac{N}{\gamma})^{-\frac{1}{2}} + \frac{d\Phi}{d\zeta}] & 0 \\
-\frac{\cos\Phi}{N}(1+\mu)\nu & -\frac{\cos\Phi}{N} D_1 (1+\frac{N}{\gamma})^{\frac{1}{2}} & 0 & -[\frac{\cos\Phi}{N} D_2 (1+\frac{N}{\gamma})^{\frac{1}{2}} - \frac{d\Phi}{d\zeta}] & [\frac{\cos^2\Phi}{N} - \frac{1}{\delta}(1+\frac{N}{\gamma})]\nu & -\frac{\cos\Phi(1-d)\sin\Phi}{N} & 0 & -\frac{\cos\Phi}{N}[\frac{D_3}{2\gamma}(1+\frac{N}{\gamma})^{-\frac{1}{2}} + \frac{d\Phi}{d\zeta}] \\
[\frac{\sin\Phi}{N} D_1 (1+\frac{N}{\gamma})^{\frac{1}{2}} - \frac{d\Phi}{d\zeta}] & -\frac{\sin\Phi}{N}(1+\mu)\nu & \frac{\sin\Phi}{N} D_2 (1+\frac{N}{\gamma})^{\frac{1}{2}} & 0 & \frac{\sin^2\Phi}{N}(1-d) & \frac{\sin\Phi\cos\Phi\nu}{N} & \frac{\sin\Phi}{N}[\frac{D_3}{2\gamma}(1+\frac{N}{\gamma})^{-\frac{1}{2}} + \frac{d\Phi}{d\zeta}] & -\frac{1}{\gamma\delta}\nu \\
\frac{\sin\Phi}{N}(1+\mu)\nu & [\frac{\sin\Phi}{N} D_1 (1+\frac{N}{\gamma})^{\frac{1}{2}} - \frac{d\Phi}{d\zeta}] & 0 & \frac{\sin\Phi}{N} D_2 (1+\frac{N}{\gamma})^{\frac{1}{2}} & -\frac{\sin\Phi\cos\Phi\nu}{N} & \frac{\sin^2\Phi(1-d)}{N} & \frac{1}{\gamma\delta}\nu & \frac{\sin\Phi}{N}[\frac{D_3}{2\gamma}(1+\frac{N}{\gamma})^{-\frac{1}{2}} + \frac{d\Phi}{d\zeta}] \\
-\frac{D_1}{N}(1+\frac{N}{\gamma})^{\frac{1}{2}} & \frac{1}{N}(1+\mu)\nu & -\frac{D_2}{N}(1+\frac{N}{\gamma})^{\frac{1}{2}} & 0 & -\frac{(1-d)\sin\Phi}{N} & -\frac{\cos\Phi\nu}{N} & -\frac{1}{N}[\frac{D_3}{2\gamma}(1+\frac{N}{\gamma})^{-\frac{1}{2}} + \frac{d\Phi}{d\zeta}] & 0 \\
-\frac{1}{N}(1+\mu)\nu & -\frac{D_1}{N}(1+\frac{N}{\gamma})^{\frac{1}{2}} & 0 & -\frac{D_2}{N}(1+\frac{N}{\gamma})^{\frac{1}{2}} & \frac{\cos\Phi\nu}{N} & -\frac{(1-d)\sin\Phi}{N} & 0 & -\frac{1}{N}[\frac{D_3}{2\gamma}(1+\frac{N}{\gamma})^{-\frac{1}{2}} + \frac{d\Phi}{d\zeta}] \\
D_4(1+\frac{N}{\gamma})^{\frac{1}{2}} & 0 & D_5(1+\frac{N}{\gamma})^{\frac{1}{2}} & -\nu & (1-d)\cos\Phi & -(1+\mu)\sin\Phi\nu & \frac{D_6}{2\gamma}(1+\frac{N}{\gamma})^{-\frac{1}{2}} & 0 \\
0 & D_4(1+\frac{N}{\gamma})^{\frac{1}{2}} & \nu & D_5(1+\frac{N}{\gamma})^{\frac{1}{2}} & (1+\mu)\sin\Phi\nu & (1-d)\cos\Phi & 0 & \frac{D_6}{2\gamma}(1+\frac{N}{\gamma})^{-\frac{1}{2}}
\end{pmatrix}
\begin{pmatrix} \bar{u}_R \\ \bar{u}_I \\ \bar{v}_R \\ \bar{v}_I \\ \bar{\phi}_R \\ \bar{\phi}_I \\ \bar{n}_R \\ \bar{n}_I \end{pmatrix} \tag{3.4}
$$

$$
\begin{pmatrix}
-C(1+\sin^2\Phi) & (M+k)\nu & -C\sin\Phi\cos\Phi & 0 & -(M-a)\sin\Phi & -(M+k)\cos\Phi\nu & 0 & 0 \\
-(M+k)\nu & -C(1+\sin^2\Phi) & 0 & -C\sin\Phi\cos\Phi & (M+k)\cos\Phi\nu & -(M-a)\sin\Phi & 0 & 0 \\
-C\sin\Phi\cos\Phi & 0 & -C(1+\cos^2\Phi) & (M+k)\nu & -(M-a)\cos\Phi & +(M+k)\sin\Phi\nu & 1 & 0 \\
0 & -C\sin\Phi\cos\Phi & -(M+k)\nu & -C(1+\cos^2\Phi) & -(M+k)\sin\Phi\nu & -(M-a)\cos\Phi & 0 & 1 \\
0 & 0 & 0 & 0 & 0 & 0 & 0 & 0 \\
0 & 0 & 0 & 0 & 0 & 0 & 0 & 0 \\
0 & 0 & 0 & 0 & 0 & 0 & 0 & 0 \\
0 & 0 & 0 & 0 & 0 & 0 & 0 & 0
\end{pmatrix}
\begin{pmatrix}
\bar{u}_R(0) \\ \bar{u}_I(0) \\ \bar{v}_R(0) \\ \bar{v}_I(0) \\ \bar{\phi}_R(0) \\ \bar{\phi}_I(0) \\ \bar{n}_R(0) \\ \bar{n}_I(0)
\end{pmatrix}
+
\begin{pmatrix}
0 & 0 & 0 & 0 & 0 & 0 & 0 & 0 \\
0 & 0 & 0 & 0 & 0 & 0 & 0 & 0 \\
0 & 0 & 0 & 0 & 0 & 0 & 0 & 0 \\
0 & 0 & 0 & 0 & 0 & 0 & 0 & 0 \\
1 & 0 & 0 & 0 & -\cos\Phi & 0 & 0 & 0 \\
0 & 1 & 0 & 0 & 0 & -\cos\Phi & 0 & 0 \\
0 & 0 & 1 & 0 & +\sin\Phi & 0 & 0 & 0 \\
0 & 0 & 0 & 1 & 0 & +\sin\Phi & 0 & 0
\end{pmatrix}
\begin{pmatrix}
\bar{u}_R(1) \\ \bar{u}_I(1) \\ \bar{v}_R(1) \\ \bar{v}_I(1) \\ \bar{\phi}_R(1) \\ \bar{\phi}_I(1) \\ \bar{n}_R(1) \\ \bar{n}_I(1)
\end{pmatrix}
=
\begin{pmatrix}
0 \\ 0 \\ 0 \\ 0 \\ \alpha_R(\nu) \\ \alpha_I(\nu) \\ \beta_R(\nu) \\ \beta_I(\nu)
\end{pmatrix}
\tag{3.5}
$$

$$
\begin{pmatrix} \frac{dw_R}{d\zeta} \\ \frac{dw_I}{d\zeta} \\ \frac{d\psi_R}{d\zeta} \\ \frac{d\psi_I}{d\zeta} \end{pmatrix} = \begin{pmatrix} -\frac{\cos\Phi}{N} D_7 (1+\frac{N}{\gamma})^{\frac{1}{2}} & \frac{\cos\Phi}{N}(1+\eta)\nu & [\frac{\cos\Phi}{N}(1-d)\sin\Phi+\sin\Phi\frac{d\Phi}{d\zeta}] & [\frac{\cos^2\Phi}{N}(1+4h\xi)\nu - \frac{1}{\delta}(1+\frac{N}{\gamma})\nu] \\ -\frac{\cos\Phi}{N}(1+\eta)\nu & -\frac{\cos\Phi}{N} D_7 (1+\frac{N}{\gamma})^{\frac{1}{2}} & [-\frac{\cos^2\Phi}{N}(1+4h\xi)\nu+\frac{1}{\delta}(1+\frac{N}{\gamma})\nu] & [\frac{\cos\Phi}{N}(1-d)\sin\Phi + \sin\Phi \frac{d\Phi}{d\zeta}] \\ \frac{D_7}{N}(1+\frac{N}{\gamma})^{\frac{1}{2}} & -\frac{(1+\eta)\nu}{N} & -\frac{(1-d)\sin\Phi}{N} & -\frac{(1+4h\xi)}{N}\cos\Phi\nu \\ \frac{(1+\eta)\nu}{N} & \frac{D_7}{N}(1+\frac{N}{\gamma})^{\frac{1}{2}} & \frac{(1+4h\xi)}{N}\cos\Phi\nu & -\frac{(1-d)\sin\Phi}{N} \end{pmatrix} \begin{pmatrix} w_R \\ w_I \\ \psi_R \\ \psi_I \end{pmatrix} \tag{3.6}
$$

$$
\begin{pmatrix} -C & (M+k)\nu & (M-a)\sin\Phi & (M+k)\cos\phi\nu \\ -(M+k)\nu & -C & -(M+k)\cos\Phi\nu & (M-a)\sin\Phi \\ 0 & 0 & 0 & 0 \\ 0 & 0 & 0 & 0 \end{pmatrix} \begin{pmatrix} \bar{w}_R(0) \\ \bar{w}_I(0) \\ \bar{\psi}_R(0) \\ \bar{\psi}_I(0) \end{pmatrix} + \begin{pmatrix} 0 & 0 & 0 & 0 \\ 0 & 0 & 0 & 0 \\ 1 & 0 & \cos\Phi & 0 \\ 0 & 1 & 0 & \cos\Phi \end{pmatrix} \begin{pmatrix} \bar{w}_R(1) \\ \bar{w}_I(1) \\ \bar{\psi}_R(1) \\ \bar{\psi}_I(1) \end{pmatrix} = \begin{pmatrix} 0 \\ 0 \\ \varepsilon_R(\nu) \\ \varepsilon_I(\nu) \end{pmatrix} \tag{3.7}
$$

Equations (3.4) and (3.5) and equations (3.6) and (3.7) for the spatial dependence of motion variables are cast into a normal form for linear boundary value problems.

The terms of the coefficient matrices of these cable dynamic equations have a complicated spatial dependence arising from the solution of the non-linear steady configuration equations. Therefore a numerical integration scheme is essential for their solution. A two part scheme is used. First, the steady configuration equations are integrated. Then, those results are used in the integration of the dynamic equations. The numerical scheme was implemented on the IBM 370/155 at the M.I.T. Information Processing Center.

Steady Configuration Solution

The equations for the steady configuration (2.19a,b) subject to the initial values at $\zeta = 0$ given by equations (2.23a,b) may be integrated by any of the standard integration schemes for a system of non-linear, first order, ordinary differential equations. Hamming's Predictor-Corrector method was used as provided by IBM (1970) in their Scientific Subroutine Package. The problem is straightforward and the choice of a particular method of integration is not crucial. The results of the steady configuration must be put into the coefficient matrix of the dynamic equations when solving them. The simplest technique is to make up a table of the values of the solution variables, tension and trail angle, as they are generated at each step. The table may be accessed with a

value of the independent variable. Later when values are needed to compute the terms in the coefficient matrices of the dynamic equations the table may be entered with a value of ζ and linear interpolation between adjacent tabular values of Φ and N used to generate the correct values. A step size should be selected which will provide accuracy consistent with the requirements of later steps in the computational scheme.

As mentioned before the results of the integration of the steady configuration equations have been considered in detail by other investigators, nevertheless, some observations are appropriate to assist in understanding the results of the investigation of the dynamic equations. Perhaps the most striking feature of the steady configuration of a towed cable is the sweeping curve it makes in space. Near the towed body, curvature is likely to be pronounced with the curve flattening as it moves nearer the tow point. Imagine a cable with no body at the end. Such a cable will have no curvature. The angle at which it tows, called the critical angle, will be found by setting $d\Phi/d\zeta = 0$ in equation (2.19a) giving the transcendental equation

$$(1-d)\cos\Phi_c = D(a_1+a_2\sin\Phi_c)\sin\Phi_c\,(1+\frac{N}{\gamma})^{\frac{1}{2}} \qquad (3.8)$$

Equation (3.8) shows that the critical angle is the angle achieved by the cable as a result of balancing its weight with viscous drag forces. Equation (2.19b) may still be integrated to give tension along the cable. The initial value of tension at $\zeta = 0$ will be zero in the absence of a body. The tension will vary linearly along the cable as long as $\gamma >> N$ which is the usual case.

Now imagine a body moving at the towing velocity. The resultant force from the body's weight and drag will also make an angle with the horizontal in general different from and certainly independent of the critical angle described above. This angle is found in equation (2.23a). When the body is attached to the cable the resultant force on the body from weight and drag must be matched by the cable which is then deformed from its linear trajectory. The effect of this body constraint is propagated up the cable toward the towpoint dying out as it goes. Therefore the greatest curvatures are found closest to the body. Equation (3.8), not to mention common sense, shows that the greater the drag the smaller the critical angle and therefore the shallower the tow for a given length of cable. Similar reasoning applies to the towed body.

In most towed body situations designers seek to minimize the length of cable necessary to attain a desired towing depth for obvious economic reasons. Therefore a premium is placed on drag reduction both of the cable fairing and the towed body. This is the principal reason for moving to the

complication of a fairing on the tow cable. The other important reason is to minimize variable drag and side force by minimizing vortex shedding effects. An additional technique frequently employed to drive a towed body deeper is to equip it with a depressor which is a hydrofoil designed to develop large downward directed lift forces. A typical steady configuration is shown in figure 3-1. When $d\Phi/d\zeta \neq 0$ due to the presence of a body at the end of the cable, the left hand side of equation (2.19b) is no longer constant and therefore N no longer varies linearly up the cable.

Dynamics Solution

Equations (2.29) and (2.31) subject to the boundary values expressed in equations (2.30) and (2.32) may be integrated similarly to the equations for the steady configurations by any of several standard integration schemes. The process is a bit more complicated because boundary conditions must be met at both ends of the integration interval instead of just at the beginning. Kerney (1971) solves his equations by a shooting technique, in which initial values are specified as the boundary values at one end, say $\zeta = 0$, with missing values supplied arbitiarily. Then the integration is carried out and the computed values at $\zeta = 1$ are compared with the desired values given by the boundary conditions. The process is repeated with different arbitrary values. Then advantage is taken of the linearity of the problem to compute the correct

Cable Parameters

d=0.175	γ=20.8	M=4.14	C=0.56	a=2.07
D=9.48	δ=0.0066	b=0.555	c=2.22	μ=0.214
k=1.035	η=3.44	ξ=0.5	h=0.5	

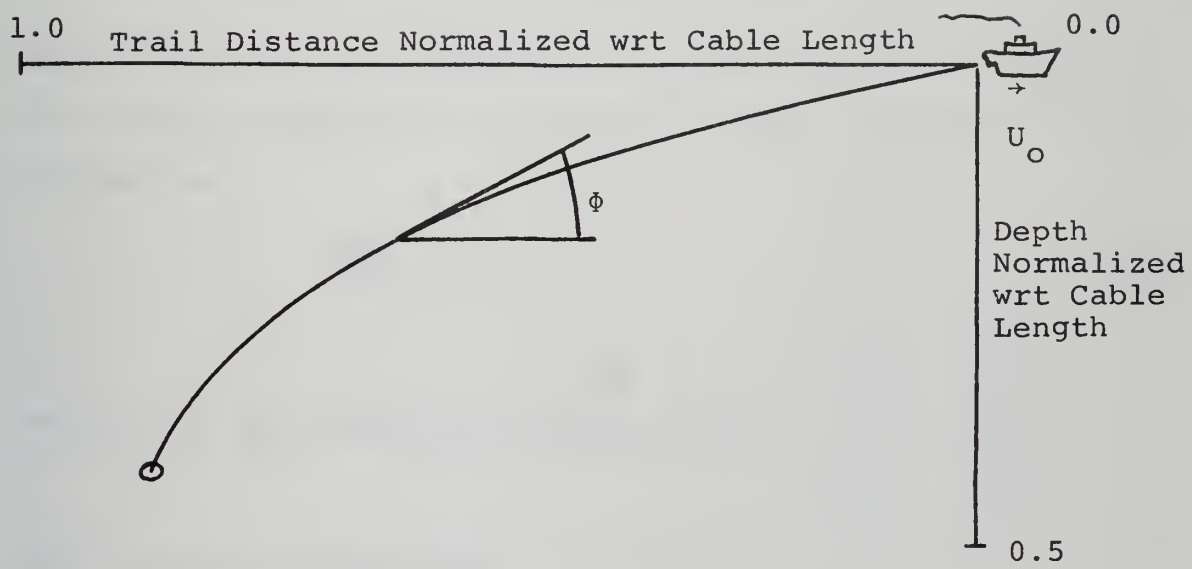

Figure 3.1

Typical Steady Configuration

missing values. A more direct approach is provided in the IBM Scientific Subroutine LBVP (an acronym for Linear Boundary Value Problem). This routine uses solutions of the adjoint problem to systematically transfer the boundary values at one boundary along the cable to the other end and then integrates the resulting initial value problem by a standard routine, again the Hamming Predictor-Corrector algorithm, HPCG.

The lateral vibration, cable dynamics equation (3.6) with associated B.C.'s in equation (3.7) may be used to show how the adjoint technique is applied in LBVP. Equation (3.6) is written as

$$\frac{d\bar{w}}{d\zeta} = A\ \bar{w} \tag{3.9}$$

where A is the coefficient matrix and $\bar{w} = \begin{pmatrix} w_R \\ w_I \\ \psi_R \\ \psi_I \end{pmatrix} = \begin{pmatrix} w_1 \\ w_2 \\ w_3 \\ w_4 \end{pmatrix}$.

The adjoint problems are

$$\frac{d\bar{W}}{d\zeta} = -A^T\bar{W} \tag{3.10}$$

with $\bar{W} = \begin{pmatrix} W_1 \\ W_2 \\ W_3 \\ W_4 \end{pmatrix}$ subject to four sets of B.C.'s

$\bar{W}|_{\zeta=1} = E_k$, k=1,2,3,4 such that for k=1, $E_1 = \begin{pmatrix} 1 \\ 0 \\ 0 \\ 0 \end{pmatrix}$ and for each

successive value of k a corresponding adjoint variable boundary value at $\zeta = 1$ is unity, all others vanishing. There are now five problems being considered: the original boundary value problem and four adjoint initial value problems, one for each value of k. The adjoint problems may now be integrated by HPCG from $\zeta = 1$ to $\zeta = 0$, thus obtaining values for the adjoint variables at $\zeta = 0$ in each of the adjoint problems.

Now $\frac{d}{d\zeta}[\sum_i W_i^k w_i] = \frac{d}{d\zeta}[\bar{W}^{kT}\bar{w}]$ where the superscript k refers to the k^{th} adjoint problem. Carrying out the differentiation on the R.H.S. and substituting from equations (3.9) and (3.10) gives $\frac{d}{d\zeta}[\sum_i W_i^k w_i] = 0$ which may be integrated giving $\sum_i W_i^k w_i|_{\zeta=1} - \sum_i W_i^k w_i|_{\zeta=0} = 0$ since equation (3.9) is homogeneous. The k^{th} adjoint B.C. at $\zeta = 1$ may be applied giving

$$\sum_i W_i^k w_i|_{\zeta=0} = w_k|_{\zeta=1} \tag{3.11}$$

There four of these equations, one for each value of k. Now the B.C.'s from the original problem are used. Suppose they are written as

$$B\bar{w}|_{\zeta=0} = 0 \tag{3.12a}$$

$$C\bar{w}|_{\zeta=1} = \bar{\varepsilon} \tag{3.12b}$$

where B and C are 2x4 coefficient matrices, that is (3.12a) and (3.12b) give two equations each. Substituting from (3.11) into (3.12b) for each value of k gives two equations now in terms of the unknowns $\bar{w}|_{\zeta=0}$ which combined with

equation (3.12a) gives four simultaneous equations in four unknowns, namely the initial values of the original problem. The coefficients of the terms in these equations are all known being combinations of the towed body parameters, the trail angle at $\zeta = 0$ and 1 obtained from the steady configuration solution, the frequency of interest and finally the solutions of the adjoint problems. These four equations may now be solved simultaneously to give the initial values for the integration of the original equations by HPCG. The transverse-longitudinal problem is handled similarly.

Solution Difficulties

The numerical scheme presented above is useful over a wide range of practical interest. It suffers, however, from a purely computational malady as frequency, cable length or viscous damping is increased. The character of the solution of equations (3.4) and (3.6) is determined by the eigenvalues of the coefficient matrices. Were the coefficients constant instead of space varying, the solution to the equations would be simply found by calculating the eigenvalues and their associated eigenvectors. Solutions would be of the form $\bar{u}(\zeta) = \sum_i \bar{c}_i e^{\lambda_i \zeta}$ where $\bar{c}_i$ are the eigenvectors and λ_i the eigenvalues. Such a procedure is in fact used in Appendix III to verify the validity of the numerical method in certain special cases wherein the coefficient matrices of equations (3.4) and (3.6) are constant. The coefficient matrices being space varying means that their eigenvalues change along the

cable but that does not affect the essence of this argument. Suppose an eigenvalue, λ_i, has a large positive real part. Then the quantity, e^{λ_i}, occurring when the B.C.'s at $\zeta = 1$ are satisfied, has a very large positive real part. Therefore arbitrary constant in c_i must be made extremely small in order to match a reasonable boundary value.

Physically, the solution consists of dying and growing waves emanating from the excitation at $\zeta = 1$. Since the towed body end of the cable is free to move about, subject to the constraint of the dynamic B.C. at $\zeta = 0$, a little of the growing solution is needed to satisfy this B.C. The growing solution eigenvalue has a positive real part and the dying solution a negative real part. As the solution is more and more damped, because the frequency, steady tow velocity, or damping coefficients have increased, or because the distributed damping along the cable has had a greater effect because the cable is longer, less and less of the growing solution is needed to satisfy the B. C. at $\zeta = 0$. If so little of the solution is needed that the value of the arbitrary constant in the eigenvector cannot be made small enough because of round-off in the computer, the numerical scheme will fail to provide a solution. Kerney (1971) apparently had similar difficulty. Practically, this difficulty seems not to be egregious since the more highly damped situations are exactly those in which the least motion is transmitted to the towed body.

In the computional scheme employed using the subroutine LBVP the difficulty manifests itself in repeated attempts to subdivide the integration step size in order to compute the solution within a small error bound. The error bound is small in order to test appropriately for loss of significance in the Gaussian elimination algorithm used to solve the set of simultaneous algebraic equations generated with the adjoint solutions for the boundary values at $\zeta = 0$.

Reducing round-off error by moving to higher precision is a way of enlarging the range of parameters for which solutions may be found using the method described in this thesis. Comparison of solution efforts using single and double precision shows that solutions which fail in single precision go forward in double precision. FORTRAN compilers are becoming available in extended precision so the range may be increased still further without resorting to the complexity of multiple precision programming. Table 3.1 shows the value of the largest positive real part of the eigenvalues of the coefficient matrix computed for the point on the cable where the largest values occur when the solution method fails in single and double precision. Table 3.1 shows that the solution proceeds for much larger positive real parts of the eigenvalues corresponding to a larger range of problem parameters, in this case frequency, when it is executed in double precision.

CABLE DATA	d=0.125 γ=2775.0 M=2.755 C=0.373 a=1.38 D=9.48 δ=0.00438 b=0.555 c=2.22 μ=0.214 k=0.69 η=3.44 ξ=0.5 h=0.5		
precision	step size	error requirement	positive real part of eigenvalue at solution failure
single	0.005	0.00001	13.43 at ν=0.175
double	0.004	0.000004	20.90 at ν=0.375

Comparison of Single and Double Precision Programs
Table 3.1

While the solution difficulty described above is troublesome, the method of solution is useful since many practical situations may still be considered. Furthermore, the difficulty can be put off to some degree by increasingly precise computation.

Future efforts directed toward more sophisticated solution schemes which avoid the above difficulty are merited. When the excitation frequency is greatly increased, the short wave length approximation will apply. That is the steady configuration trail angle and tension will change slowly over a wave length so the approximation is made that they are constant over a range of several wave lengths. The WKBJ method (cf. Morse and Feshbach (1953)) then applies. Using the same approximation Milgram (1971) suggests that a Green's function approach will work. Another useful line of investigation might be to look for ways to control the growing exponential solution in the numerical scheme, perhaps by segmenting the integration range in some fashion.

Chapter 4

RESULTS

The utility of the formulation and solution scheme for towing cable dynamics presented above can be demonstrated by applying it to a plausible cable design and examining the results. First a standard reference spectrum of tow point motions is prescribed. For the results described in this chapter the towpoint translational perturbation velocities in the x_o, y_o, z_o coordinate system are specified. The amplitudes of these perturbation velocities are unity when normalized with respect to the tow velocity U_o. A typical input perturbation is $\hat{u}_o/U_o = \delta\hat{u}/U_o = 1 \cos\nu\tau$. Because the system described is linear the results for any arbitrary spectrum may be readily obtained from the results for this flat spectrum with a normalized amplitude of unity. Second, this disturbance is applied to a basic towing cable and body design which is representative of real towing situations. Appendix IV contains a description of this system and shows how the non-dimensional parameters were obtained. The basic trial cable design envisions towing a 40 in. diameter sphere at 16 ft. per sec. with a 1200 ft. steel cable.

The greatest interest in these matters is in the motion of the towed body and in the largest unsteady values of tension in the cable. Such values are calculated and presented graphically. However, motions and tension anywhere along the cable could be determined as well. The amplitude of the

motions is of more consequence than phase so only amplitudes are presented, again normalized with respect to steady tow velocity U_o for the resulting velocities or with respect to the weight in air of the entire cable for the tensions. Furthermore, the output velocities have again been transformed from the cable coordinate system x, y, z back to the locally vertical system x_o, y_o, z_o via the transformation in equation (2.2).

After the motions and tensions of the basic cable are established, significant parameters are varied over a wide range. Cable lengths from 300 to 1800 ft., steady tow velocities from 0.1 to 48 ft. per sec., and moduli of elasticity from 2.5×10^4 psi to virtually inextensible are considered. Variations were made one parameter at a time using the basic cable as a reference. Other parameters could also be varied and indeed probably would be in a design situation. Length and velocity variations seem most significant since for any design these parameters are likely to vary during the use of the system. Modulus of elasticity was varied because the predicted results of moving to springier cables are particularly interesting. Finally, researchers have frequently ignored the added mass of the cable in previous investigations so the basic cable was considered sans cable added mass and results compared.

A physical feel for a complicated problem like this may be elusive. But the idea of a damped oscillator is basic to the physics of this interaction and so the natural frequencies

are of interest. Bearing in mind that this idea is not being applied as a tool of analysis but rather as a way of understanding, natural frequencies of various idealisations of the problem are calculated, compared to sample results and discussed.

Basic Cable System

The results from applying the solution method to the basic system are shown in figure 4.1. The magnitude of the unsteady tension n_m, at the tow point where it is greatest rises approximately quadratically with increasing frequency in the higher frequency range. This is expected for the nearly inextensible steel cable and reflects the increasing inertial forces at higher frequencies. The magnitude is largest at the tow point because the cable there must carry the load of its entire length and the body as well. The amplitude of lateral velocity w_{om} decays rapidly with increasing frequency showing the effect of heavy viscous damping. v_{om} and u_{om} cannot decay substantially because they are in the plane of the steady configuration and the near inextensibility of the cable implies that most of the tow-point motion will be transferred to the body. Some energy is removed from the cable by the viscous damping but most is transmitted down the cable to the body. The relation between the amplitude of the vertical and horizontal components seems to be a strong function of the relation between the trail angle at the tow-point and towed body, as will be apparent in later figures.

Cable Parameters

d=0.125	γ=4160.0	M=4.14	C=0.56	a=2.07
D=9.48	δ=0.0066	b=0.555	c=2.22	μ=0.214
k=1.0315	η=3.44	ξ=0.5	h=0.5	

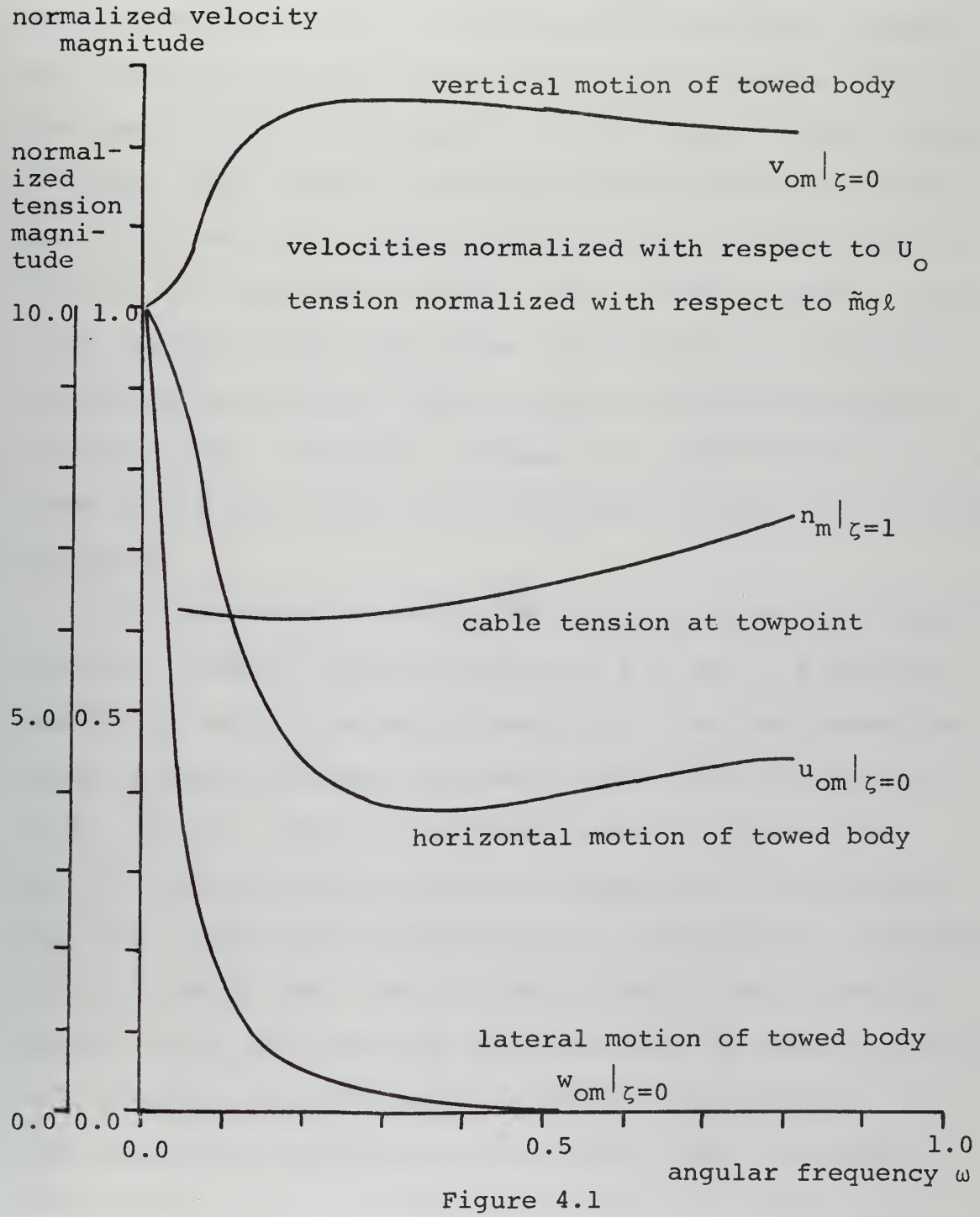

Figure 4.1

Motions and Tensions - Basic Cable

Variation of Cable Parameters

The results of varying the length of the cable are shown in figures 4.2 and 4.3. Table 4.1 shows the values of the cable parameters used. As cable length increases, motions are diminished because there is more total damping, that is the same drag per unit length is acting over a longer length of cable. The vertical and horizontal motions tend toward a limit defined by the relation of the angle of the resultant force at the towed body and the cable critical angle. As the cable becomes longer and longer the angle at the towpoint approaches the critical angle, and so the motions approach a limiting case. As length increases the lateral motion of the towed body becomes more and more rapidly damped with increasing frequency.

The variations of steady tow velocity give more dramatic results. Table 4.2 and figures 4.4, 4.5, and 4.6 show the results of varying velocity from 0.1 ft. per sec. where the cable is nearly hanging vertically below the tow point to 48 ft. per sec. where it is towing nearly horizontally. The two striking features are the appearance of resonances when the linearized viscous damping is quite small corresponding to U_o being small and the way in which the predominant motion shifts from vertical when the cable is hanging vertically to horizontal when the cable is extended horizontally. In both cases the vibrations normal to the cable are being damped while the longitudinal vibrations are transferred directly to the towed body. The lateral motion at the smallest towing velocity of 0.1 fps may be in error at the

ℓ ft.	γ	M	C	a	δ	k
300	16640.0	16.56	2.240	8.28	0.0264	4.14
600	8320.0	8.28	1.120	4.14	0.0132	2.07
900	5550.0	5.52	0.746	2.76	0.00879	1.38
1200	4160.0	4.14	0.560	2.07	0.0066	1.03
1500	3330.0	3.31	0.448	1.656	0.00528	0.828
1800	2775.0	2.755	0.373	1.380	0.00438	0.690

Changes from Basic Cable Parameters for Length Variations

Table 4.1

U_o f.p.s.	C	D	δ
0.1	0.0000219	0.00037	0.00000026
1	0.00219	0.037	0.000026
3	0.01967	0.333	0.000235
6	0.0786	1.331	0.000938
12	0.314	5.33	0.00375
18	0.706	11.92	0.00843
24	1.256	21.30	0.0150
48	5.020	85.30	0.0599

Changes from Basic Cable Parameters for Tow Velocity Variations

Table 4.2

E psi x 10^6	γ
∞	99999999.0
10	2080.0
5	1040.0
0.5	104.0
0.1	20.8
0.05	10.4
0.025	5.2

Changes from Basic Cable Parameters for Elasticity Variations

Table 4.3

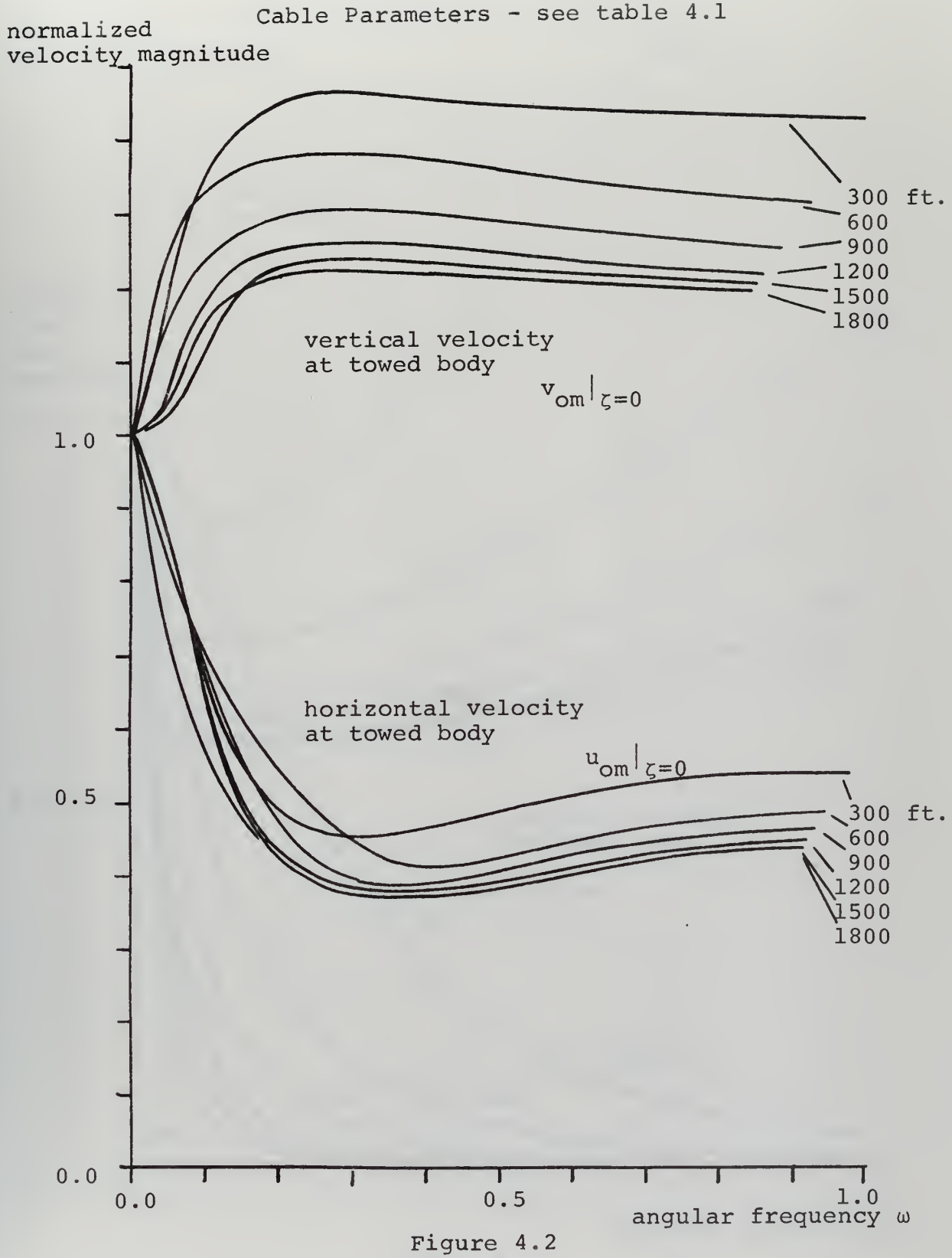

Figure 4.2

Vertical and Horizontal Motion - Length Variation

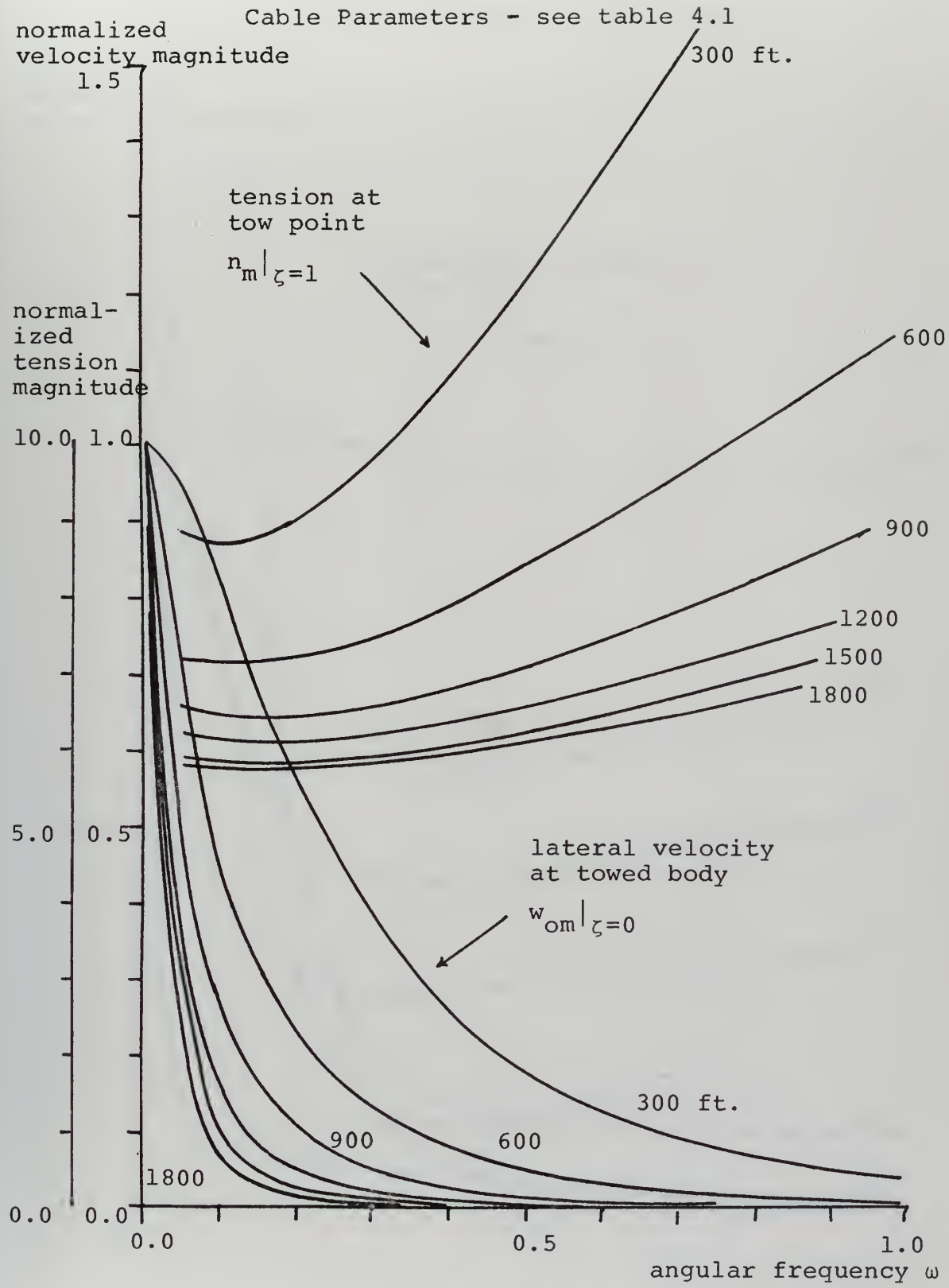

Figure 4.3

Lateral Motion and Tension - Length Variation

Cable Parameters - see table 4.2

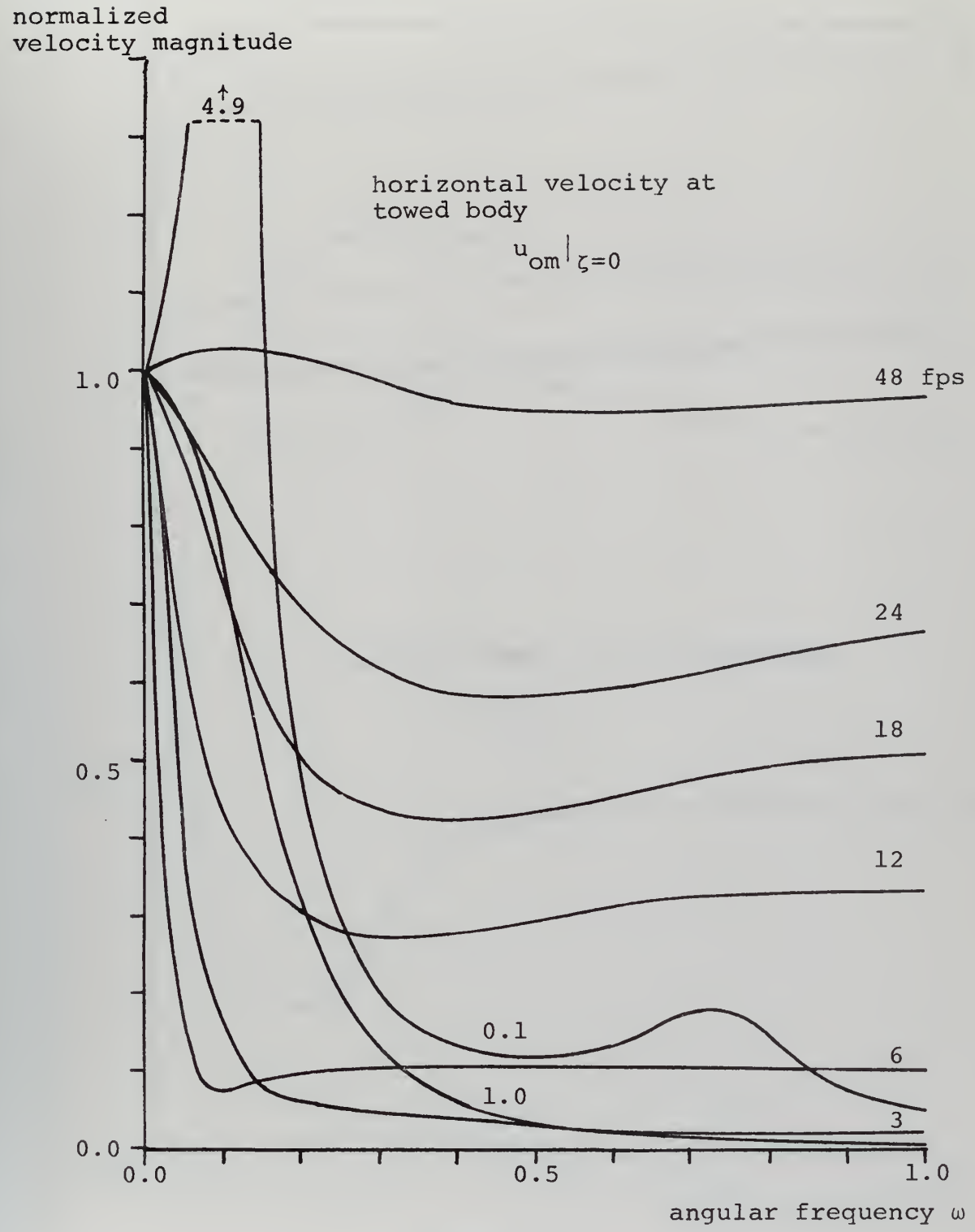

Figure 4.4

Horizontal Motions - Steady Velocity Variation

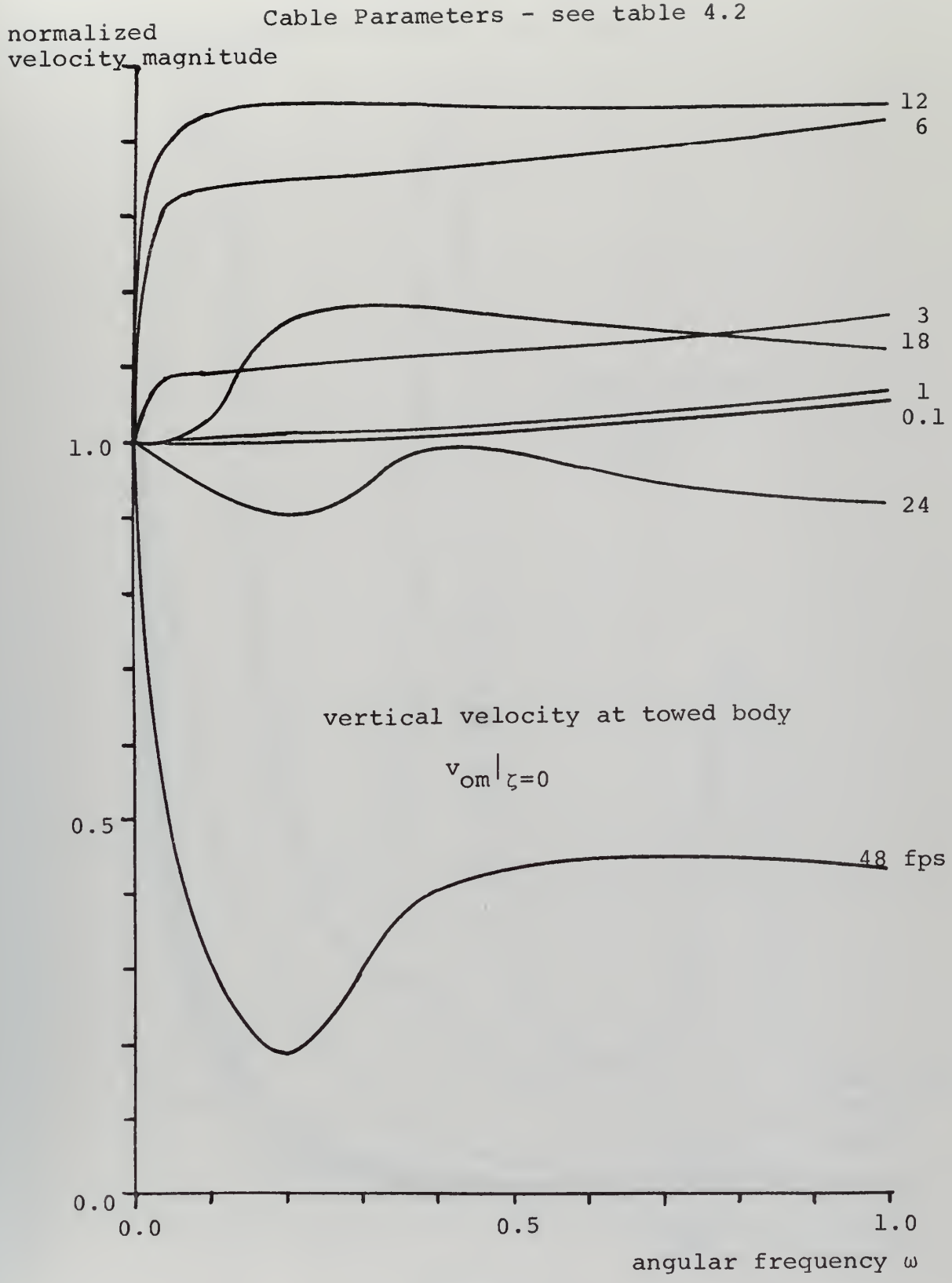

Figure 4.5

Vertical Motions - Steady Velocity Variation

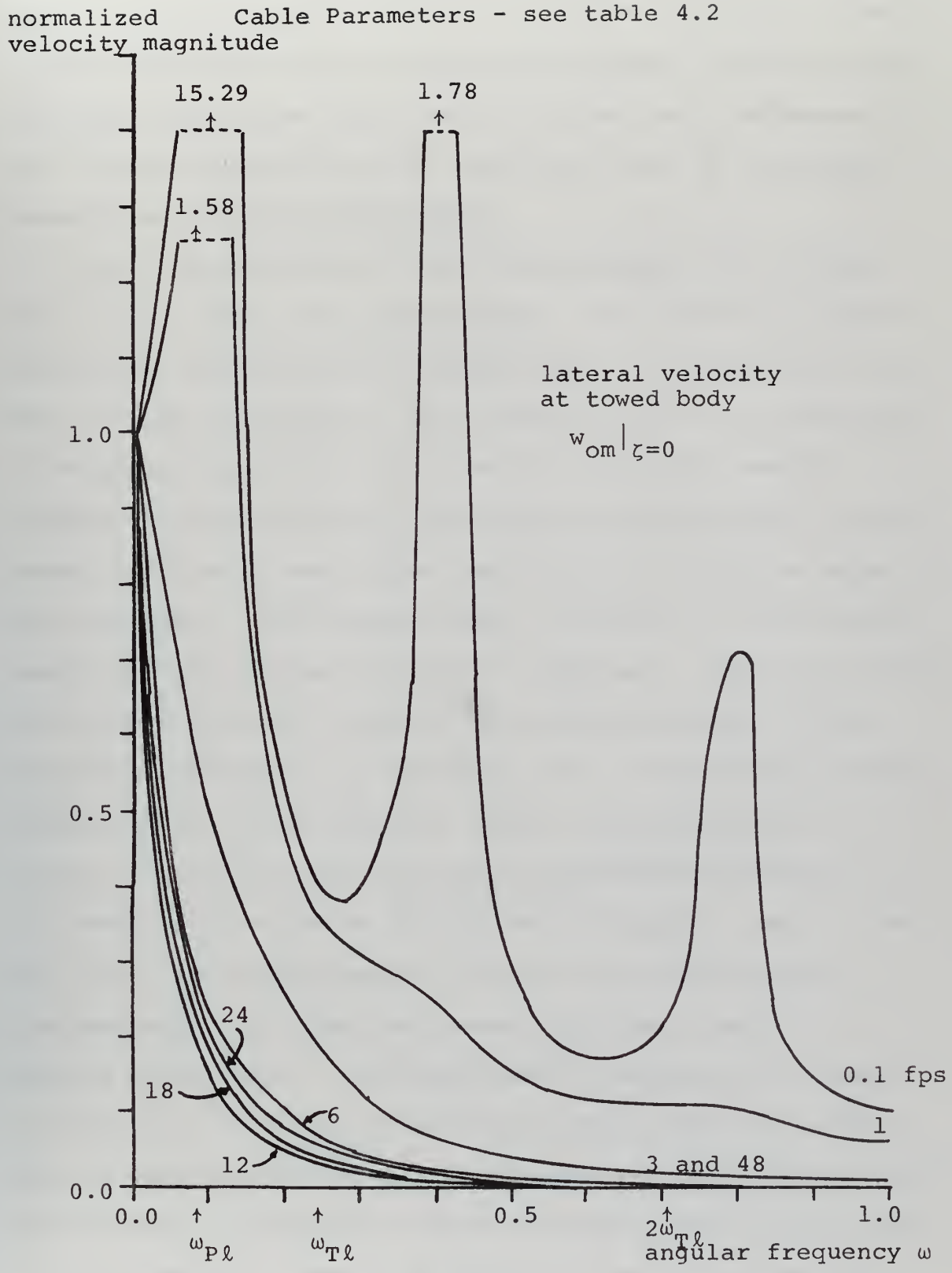

Figure 4.6

Lateral Motions - Steady Velocity Variation

higher frequencies because the low reduced frequency criterion in the derivation of the lateral hydrodynamic forces is being violated. Note that the shapes of curves near resonances in the various figures are only approximate due to the narrow bandwidths sometimes encountered.

Most investigators of tow cable dynamics have assumed that the tow cable was inextensible. This certainly seems a reasonable assumption for a steel cable. Huffman (1970), however, recognized that if a time domain solution by the method of characteristics is to be attempted the cable must be assumed extensible so that the initial value problem is well-posed, an unusual case where complicating the problem makes it more tractable. The results shown in figure 4.7 are another reason why cable extensibility is important. The more elastic the cable the less it couples the surface motions to body. Potential resonances are unlikely to be a significant problem because there is considerable viscous damping present. In figure 4.7 vertical and horizontal normalized velocities of the towed body are shown for cables with moduli ranging from 2.5×10^4 psi to inextensible and the associated natural frequencies for an idealized mass-spring oscillator of similar proportions. Associated cable parameters are shown in table 4.3. For the more elastic cables there is a great deal of coupling between the transverse and longitudinal modes of vibration. Transverse damping is much greater than longitudinal damping. Energy is coupling from the stress waves into the transverse tension waves and then being damped out

Cable Parameters - see table 4.3

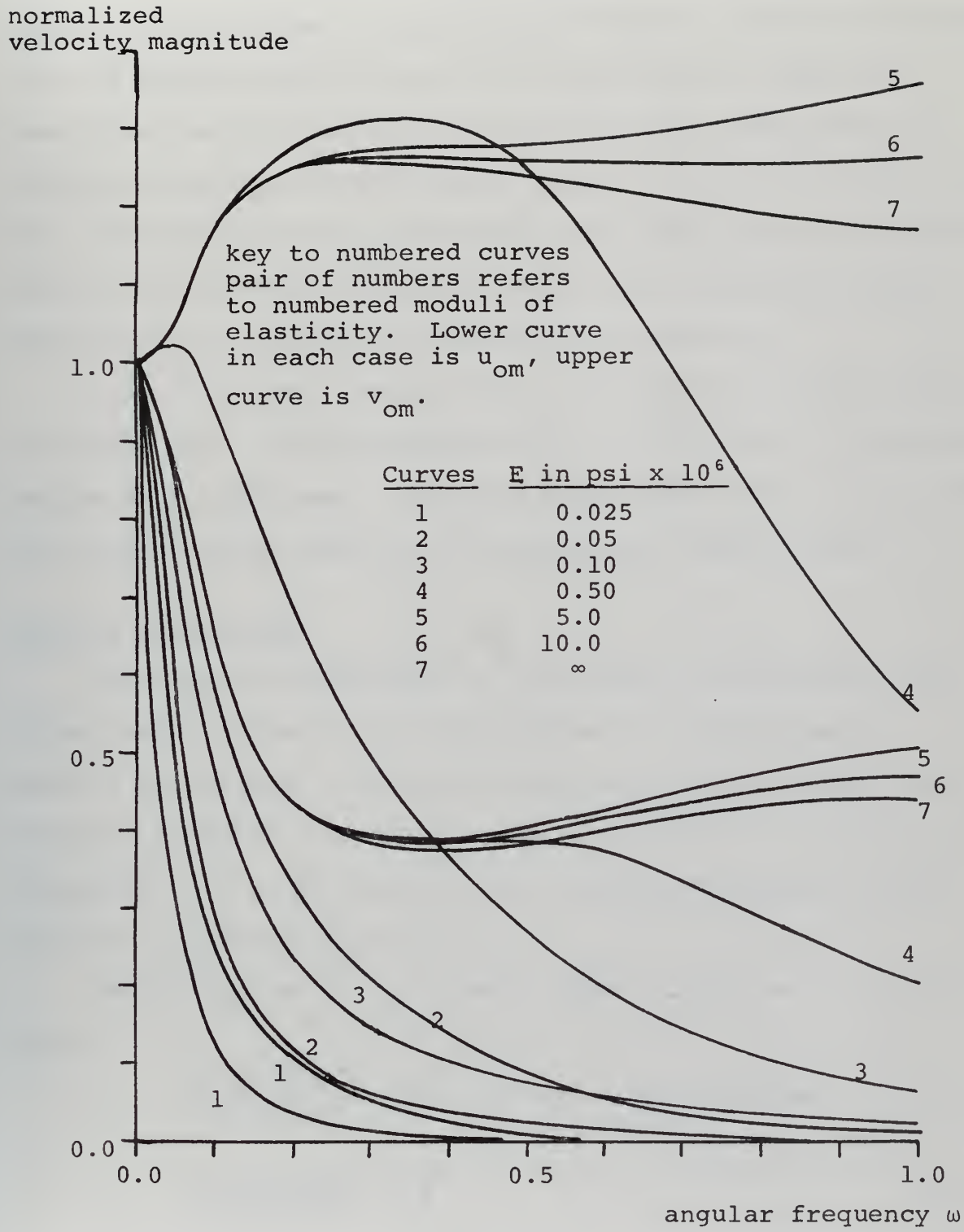

Figure 4.7

Horizontal and Vertical Motions - Elasticity Variation

because of the viscous effects. Bringing the natural frequencies of the longitudinal stress waves and the transverse tension waves into the range of the forcing frequency facilitates damping and reduces the motions of the towed body. Figure 4.7 shows how the perturbation velocities of the towed body are greatly attenuated for the lower values of modulus of elasticity. This process might be abetted in a real system by inserting springs at intervals along the cable or by choosing a cable material with a fairly low modulus of elasticity.

A solution was generated for the basic cable system without added mass. Results were within 1.0% of those of the basic system with added mass. Ignoring cable added mass is justified for cable systems similar to the basic one studied here.

Natural Frequencies

The natural frequencies of the modes of oscillation for three idealizations of the cable dynamics problem may be readily calculated. The first such idealization is that of a compound pendulum. Ignoring viscous effects on the cable and considering it to be straight, the linearized pendulum equation for transverse motions is

$$(M+k+\tfrac{1}{3}(1+\mu))\tilde{m}\ell^3\ddot{\phi} + (N(0)\tilde{m}g\ell^2 + \tfrac{1}{2}\tilde{m}g\ell^2 \sin\Phi)\phi = 0 \qquad (4.1)$$

giving

$$\omega_{Pt} = \sqrt{\frac{N(0)+\sin\Phi/2}{M+k+\frac{1}{3}(1+\mu)}}\sqrt{\frac{g}{\ell}} \quad \text{and for lateral motions} \qquad (4.2)$$

$$\omega_{P\ell} = \sqrt{\frac{N(0)+\sin\Phi/2}{M+k+\frac{1}{3}(1+\eta)}}\sqrt{\frac{g}{\ell}} \qquad (4.3)$$

where the restoring force of the pendulum is composed of gravitational forces on cable and body and viscous drag forces on the body. A second idealization is to suppose that the cable is a straight stretched string with supports at each end offering infinite impedance, subject to constant tension and again that viscous effects are negligible. Then the appropriate equation is the wave equation and the well known results (cf. Morse (1948)) for the fundamental natural frequencies of transverse and lateral motion are

$$\omega_{Tt} = \pi \sqrt{\frac{N(o)}{(1+\mu)}} \sqrt{\frac{g}{\ell}} \quad \text{and} \quad \omega_{T\ell} = \pi \sqrt{\frac{N(o)}{(1+\eta)}} \sqrt{\frac{g}{\ell}} \qquad (4.4,5)$$

Finally the extensibility of the cable gives rise to longitudinal stress waves which cause the cable system to resemble a mass spring oscillator, the natural frequencies of which may be calculated from the Rayleigh method (cf. Timoshenko and Young (1955)) to give

$$\omega_s = \sqrt{\frac{\gamma}{(M+k+\frac{1}{3})}} \sqrt{\frac{g}{\ell}} \quad \text{for a spring constant } K = \frac{AE}{\ell} \qquad (4.6)$$

again ignoring viscous effects on the cable and assuming it to be straight. Figures 4.8 and 4.9 show the consequences of allowing the fairing drag coefficient of the basic cable to vanish. The appropriate natural frequencies are shown for comparison. Figure 4.10 shows the horizontal and vertical velocities at the towed body for a similar situation except with a rather small modulus of elasticity. Comparing figure

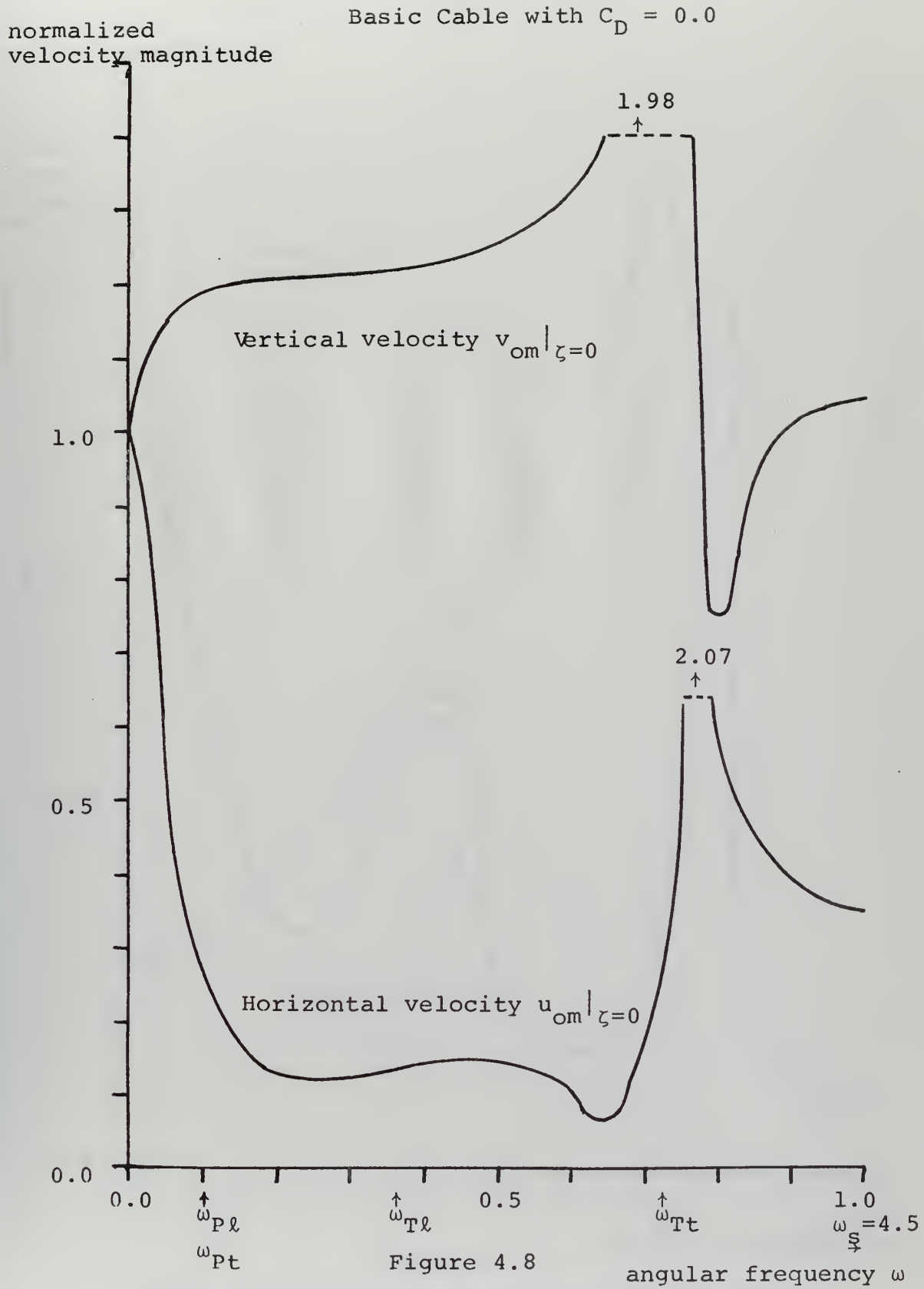

Figure 4.8

Horizontal and Vertical Motion with C_D = 0.0

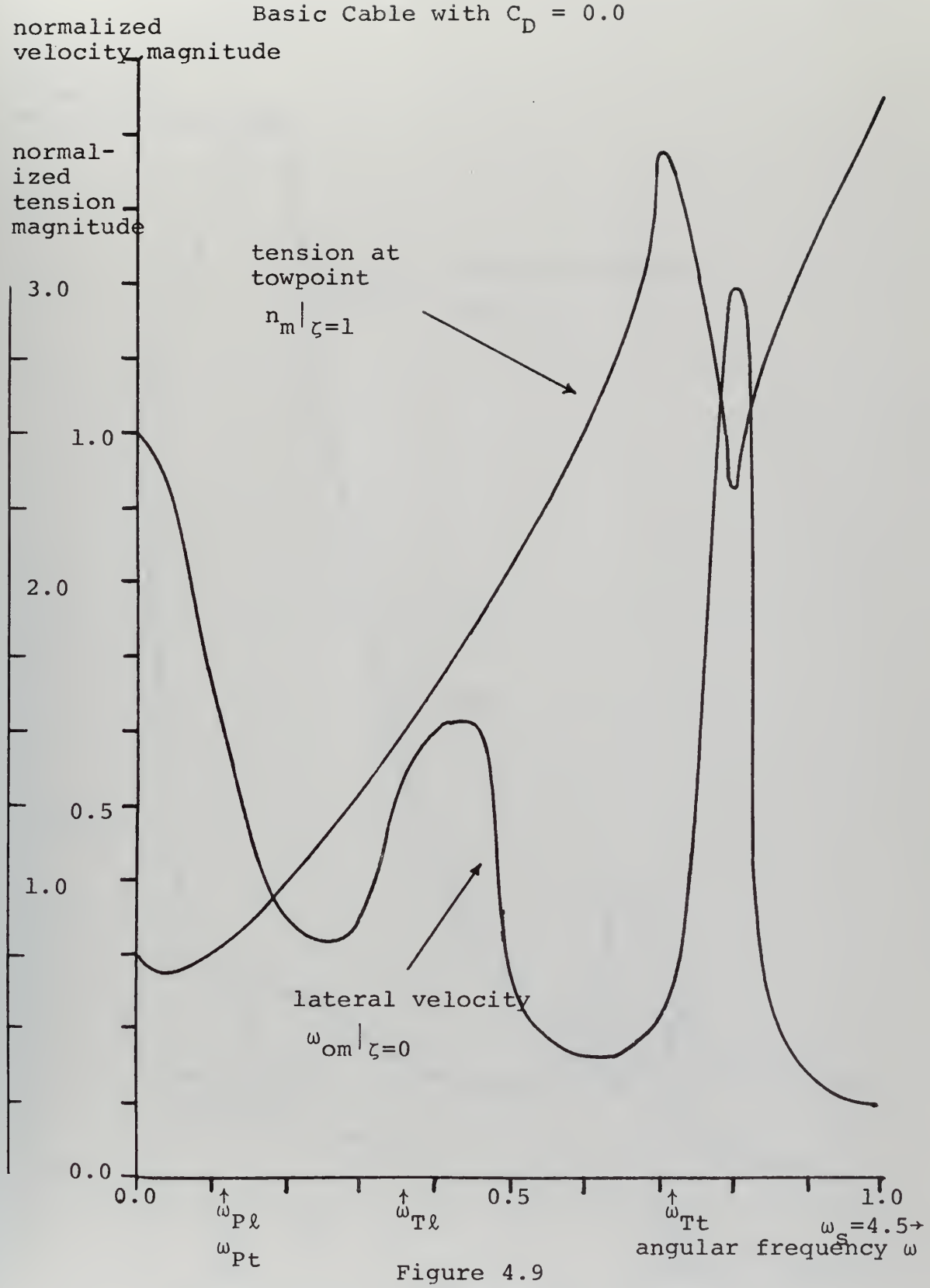

Figure 4.9

Lateral Motions and Tension with C_D = 0.0

Basic Cable with $E = 0.05 \times 10^6$ psi, $C_D = 0.0$

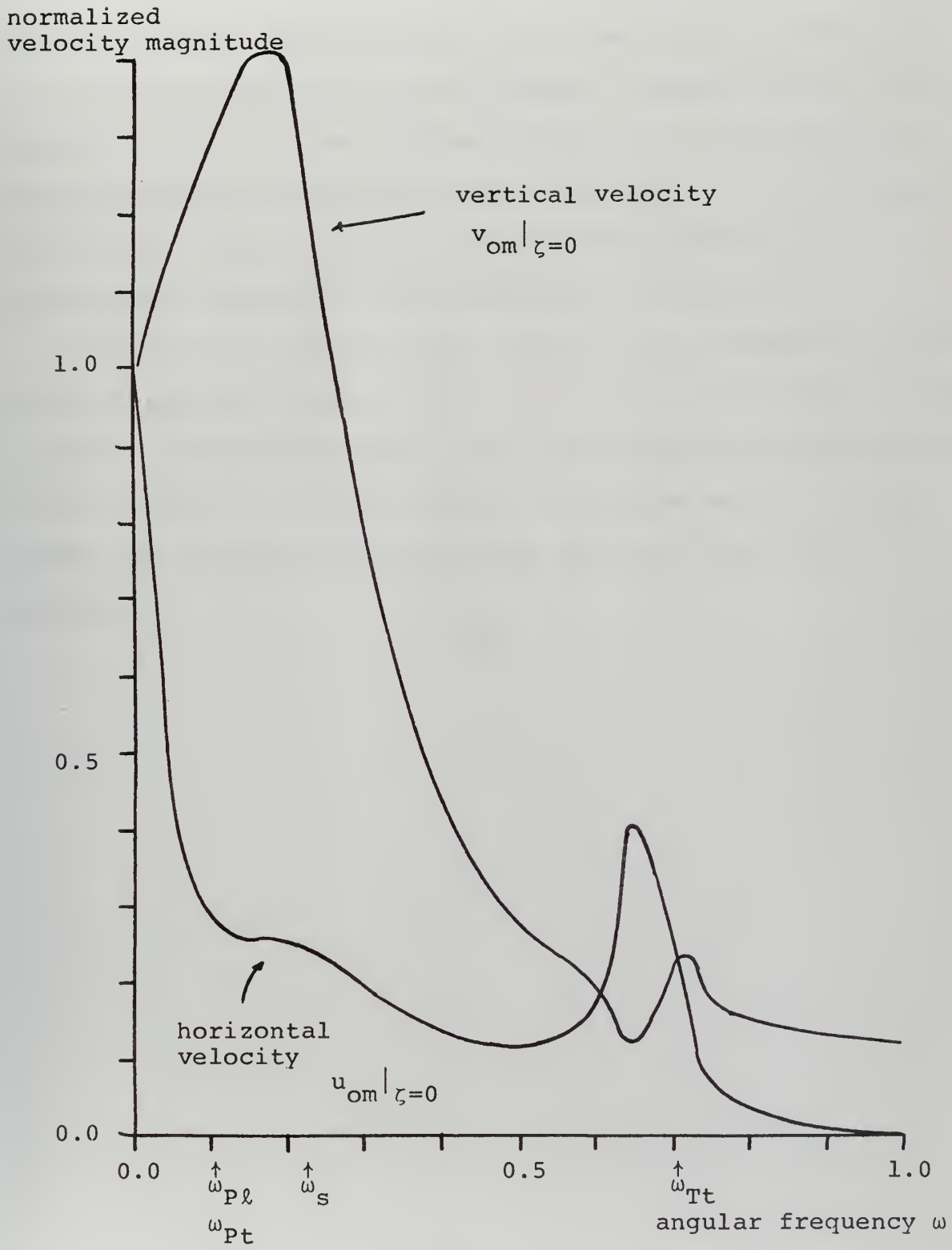

Figure 4.10

Horizontal and Vertical Motions - Very Elastic, $C_D = 0.0$

4.10 with 4.7 shows the effect of heavy viscous damping distributed along the cable. In the case shown in figure 4.10 there is viscous damping only on the towed body so modified resonancesare apparent in the frequency response curves. In figure 4.7 for the same modulus of elasticity the damping is very large and the resanances have vanished. Even in figure 4.10 though, the advantage of reduced cable modulus in limiting the motions of the towed body is apparent.

Figures 4.8, 4.9 and 4.10 indicate that the basic motions of the system are those of various simple harmonic oscillators coupled in complicated ways. When the fairing drag coefficient is restored to a reasonable value the system becomes heavily damped and resonant behavior at the natural frequencies vanishes.

Chapter 5

CONCLUSION

Design Impact

The results of this thesis may be summarized by mentioning their possible impact on the design of a towed cable system. The first result is a formulation and a method of analysis which may be easily implemented, using the FORTRAN Scientific Subroutine Package. The formulation is complete considering motions in three dimensions with a faired, extensible cable. The method allows the designer to use, directly, existing studies of ship motions in the frequency domain. Using the formulation and method the designer can find the towed body motions for given tow-point motions. The difficulty with the method is its susceptibility to overflow on the computer caused by the round-off error interacting with the growing exponential solution. This difficulty is mitigated by three factors: it is associated with increasing viscous damping and does not foreshadow any reasonance phenomenon, it may be put-off by employing more precise computation, and the range of application of the method already includes many practical designs. A second result is that fairing added masses are not important and may be ignored in typical designs without appreciable change in resulting motions. Nevertheless the formulation of cable fairing hydrodynamics of Appendix I is available. A third result is that designers may use fairly elastic cables and take advantage of the heavy viscous damping to minimize motions by creating a system in which the fundamen-

tal natural frequencies of transverse tension waves and longitudinal stress waves are small and are in the range of excitation by the tow point motions.

Suggestions for Future Work

The present need in cable dynamics is for experiments to test the various studies which have been performed. Experiments are needed in two areas, cable system dynamics as formulated in the body of this thesis and the unsteady hydrodynamics of fairings as formulated in Appendix I. Froidevaux (1968) has devised a scheme using an inertial platform to measure towed body motions which may serve as a useful start. The point is that the theory of this thesis and its antecedents have not been systematically evaluated by experiment except for the steady drag forces on the cables and the steady configurations.

Theoretical work is needed to compare the method of characteristics solutions of Schram and Reyle (1968) and Huffman (1970) with the frequency domain solutions of Kerney (1971) and of this thesis. A general formulation of the unsteady hydrodynamics of cable fairings in three dimensions is needed to replace the compound approach of Appendix I. Finally more general dynamic boundary conditions need to be developed to handle the case of a small tow ship and a large body where motions of the body affect motions of the tow ship and cases where the towed body is a more general shape than the sphere employed in this thesis.

Appendix I

HYDRODYNAMICS OF CABLE FAIRINGS

Introduction

No general formulation of the hydrodynamics of cable fairings exists. Previous investigators have largely confined their attention to the drag on a fairing resulting from a steady flow co-planar with the configuration of the cable. The problem of interest in these investigations was to find the drag forces normal and tangential to the fairing as a function of the trail angle, that is the angle of inclination of the fairing to the inflow velocity vector. Most investigators have developed loading functions. These functions are the normal and tangential drag forces normalized with respect to the drag force on the fairing when the trail angle is 90°. Casarella and Parsons (1970) present most of the significant results in a table of loading functions for faired cables. The usual approach has been to conduct experiments and then fit a curve through the data. Because the normal and tangential drag components are basically related to the squares of the normal and tangential velocity components, the usual effort is directed at constructing curves from combinations of sines and cosines of the trail angle. Two investigators, Choo (1970) and Calkins (1970), have attempted theoretical formulations of the loading functions although their methods still require some experimental input.

A more comprehensive formulation of cable fairing hydrodynamics than discussed above is necessary in an investigation of the dynamics of a faired cable in a towed system undergoing motion in three dimensions. An understanding of a three-dimensional unsteady problem as opposed to a two-dimensional steady problem is required. Added mass as well as viscous effects and the effects of motions out of as well as in the plane of the steady tow configuration must be considered. In lieu of a general formulation which may be quite difficult the following piecemeal approach has been used to understand the hydrodynamics of a cable fairing segment undergoing unsteady motions in three dimensions. The contributions of added mass to the forces and moments on the fairing segment are written following Imlay (1961). The loading function formulation of the in-plane viscous drag forces is assumed to apply to the unsteady case. The out of plane added mass and viscous forces are calculated from thin wing theory following Robinson and Laurmann (1952) after imposing some additional restrictions on the fairing. These results are then superposed to give forces and moments on the cable fairing segment. Unfortunately there are no experimental results available with which to test the compound theory described above.

Before proceeding to a detailed discussion of the compound hydrodynamic theory of cable fairing segments some simple assumptions are made about the attachment of cable fairing segments to the cable. The fairing is assumed to be attached to the cable by a frictionless bearing such that

forces are communicated to the cable but moments are not. For most fairing designs this is an excellent assumption for forces normal to the cable, less so for tangential forces. In most cases a fairing is somewhat free to slide along the cable and is only restrained from doing so by the proximity of adjacent segments. In a few designs segments are attached to collars fixed to the cable and the above assumption is then also correct for tangential forces. In a few cases not considered in the following theory fairings are bonded into the structural element of the cable so that moments exerted on the fairing about the cable axis are directly transmitted to the cable. As shown by Abkowitz (1965, 1967) these designs are subject to a kind of flutter instability and can apparently also lead to remakrable kiting effects. However, in many designs, probably to avoid the expense of attaching collars to the cable to support each fairing segment separately, adjacent segments are free to bunch together or are prevented from bunching by a flexible separator between segments. Either way a moment-side force coupling might be envisioned in so far as a segment is prevented from aligning with the local flow. In fact this complicated kind of attachment might be modeled as a pair of coupled cable dynamic problems, one for the structural cable and one for the fairing treated as a different cable with coupling through the transmission of normal forces from fairing to structural cable. Such an adventure awaits a future investigator.

Figure I-1 shows a typical fairing segment, associated cable and a coordinate system with origin on the centerline of the cable. A moderate simplification of algebra results later if the cable radius is assumed small compared to the chord length of the fairing so that the y axis of the coordinate system lies essentially along the leading edge of the fairing. The fairing is assumed to be symmetrical about its centerline plane. Real cable fairings are designed to be symmetrical but sometimes acquire a permanent set from being wound on a winch drum, producing a slight asymmetry. Adjacent segments are assumed to be infinitesimally far apart so that there are no gaps in the fairing. Actually gaps will exist and some complicated flow will go on in the gaps. None of the above assumptions about the attachment of the fairing to the cable is thought to cause significant disparity between theoretical and actual performance of the towed cable systems.

Added Mass

The added mass tensor appropriate for the arbitrary translations and rotations of the differential fairing segment in the cable coordinate system with its origin at the segment mid-plane, as shown in Figure I-2, is given below. The segment length ds is large compared to the chord of the fairing but small compared to the radius of curvature of the cable. The notation of Imlay (1961) is used in which each term is a hydrodynamic force or moment derivative per unit length of fairing with respect to the subscripted variable. Terms which

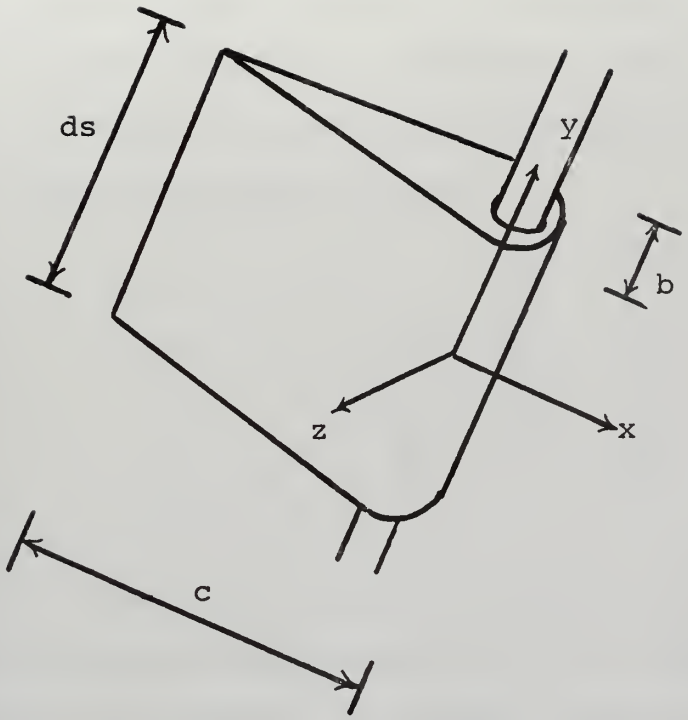

Figure I-1

Typical Fairing Segment

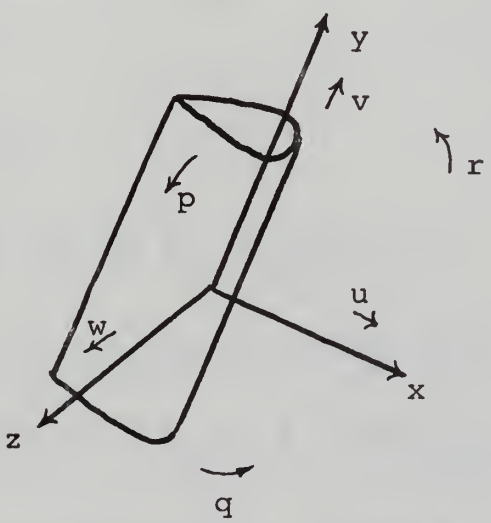

Figure I-2

Rotational and Translational Velocities of the Fairing Segment

vanish do so either because of the geometrical symmetry of the fairing segment about its centerline plane and about its mid-plane or because the fairing is continuous in the y direction of the cable coordinate system.

$$\begin{matrix} X_{\dot{u}} & 0 & 0 & 0 & 0 & 0 \\ 0 & 0 & 0 & 0 & 0 & 0 \\ 0 & 0 & Z_{\dot{w}} & 0 & Z_{\dot{q}} & 0 \\ 0 & 0 & 0 & K_{\dot{p}} & 0 & 0 \\ 0 & 0 & M_{\dot{w}} & 0 & M_{\dot{q}} & 0 \\ 0 & 0 & 0 & 0 & 0 & N_{\dot{r}} \end{matrix} \qquad \text{(I-1)}$$

where X, Y, and Z are forces in the x, y, and z directions and K, M, and N are moments about the x, y, and z axes respectively. The forces and moments on a rigid, isolated fairing segment of length ds retaining only linear terms in the perturbation variables are then given by

$$\begin{aligned} X^{(a)} &= X_{\dot{u}}\, ds\, \dot{\hat{u}} \\ Y^{(a)} &= X_{\dot{u}}\, ds\, u^*\, \dot{\hat{r}} \\ Z^{(a)} &= Z_{\dot{w}}\, ds\, \dot{\hat{w}} + Z_{\dot{q}}\, ds\, \dot{\hat{q}} - X_{\dot{u}}\, ds\, u^*\, \hat{q} \\ K^{(a)} &= Z_{\dot{w}}\, ds\, v^*\, \hat{w} + Z_{\dot{q}}\, ds\, v^*\, \hat{q} + K_{\dot{p}}\, ds\, \dot{\hat{p}} \\ M^{(a)} &= Z_{\dot{q}}\, ds\, (\dot{\hat{w}} - u^*\hat{q}) + M_{\dot{q}}\, ds\, \dot{\hat{q}} - (Z_{\dot{w}} - X_{\dot{u}})\, ds\, u^*\, \hat{w} \\ N^{(a)} &= -X_{\dot{u}}\, ds\, (u^*v^* + u^*\hat{v} + v^*\hat{u}) + N_{\dot{r}}\, ds\, \dot{\hat{r}} \end{aligned} \qquad \text{(I-2a-f)}$$

Some simplifications result from considering how the above hydrodynamic forces and moments on a fairing segment from added mass interact with the cable. Equations (I-2d) and (I-2f) give moments about axes normal to the cable element and are therefore bending moments. The basic cable assumption is that bending moments are negligible. For bending moments to contribute to cable deformation the moment at any point in the cable must be finite, that is of 0(1). Equations (I-2d) and (I-2f) give bending moments of 0(ds) and therefore may be ignored in considering the cable dynamics.

Equations (I-2a) and (I-2b) will be combined with the results of considering viscous drag forces to give the components of the total hydrodynamic forces on the cable in the x and y directions. $X_{\dot{u}}$ may be estimated by assuming that the added mass is similar to that of an elliptical section of the same thickness. This assumption gives $X_{\dot{u}} = -\frac{1}{4}\rho\pi b^2$ when b is the maximum breadth of the fairing.

Equations (I-2c) and (I-2e) will be used in conjunction with the results from thin wing theory to give the contribution to lateral forces and moments due to added mass caused by the thickness of the fairing. These corrections to the thin wing theory will be the terms in equations (I-2c) and (I-2e) involving $X_{\dot{u}}$.

Loading Functions

Viscous drag forces on cables have customarily been given by investigators in the form of loading functions. In the two-dimensional steady problem as shown earlier in this paper the dependent variables are tension and trail angle. The trail angle gives the orientations of the cable relative to the steady flow. If the cable is oriented normal to the flow corresponding to a trail angle of 90° the drag force will be given by

$$\bar{R} = -C_D \tfrac{1}{2}\rho\, c\, ds\, \bar{V}|\bar{V}| \tag{I-3}$$

where C_D is a drag coefficient depending on Reynold's number, C the chord length of the fairing, ds the span of the fairing segment and $\bar{V}$ the fairing velocity vector. For the equations of motion of the cable element the normal and tangential components of the drag force are of interest. As the cable is inclined to the flow these components will vary as functions of the inclination angle, θ. Normal and tangential loading functions may then be defined as

$$f_n = \frac{D_{normal}(\theta)}{-R} \tag{I-4a}$$

$$f_t = \frac{D_{tangential}(\theta)}{-R} \tag{I-4b}$$

where f_n and f_t are the normal and tangential loading functions, D_{normal} and $D_{tangential}$ are the normal and tangential components of the viscous drag force and $R = |\bar{R}|$. f_n and f_t have

been measured experimentally and expressed in terms of sine and cosine series. Casarella and Parsons (1970) give the forms of f_n and f_t which have been developed by various investigators. The theoretical formulations of Calkins (1970) and Choo (1970) are of interest but are no more useful in the development of the theory of this paper than the experimental results. In the absence of new definitive experimental results for a variety of fairing shapes and Reynold's numbers the loading functions developed by Whicker (1957) seem as relevant as any. These loading functions are

$$f_n = a_1 \sin \theta + a_2 \sin^2 \theta \qquad \text{(I-5a)}$$

$$f_t = b_1 \cos \theta + b_2 \cos^2 \theta \qquad \text{(I-5b)}$$

where the coefficients are $a_1 = 1 - \frac{b}{c}$, $a_2 = \frac{b}{c}$, $b_1 = 0.386 - 0.303 \frac{b}{c}$, $b_2 = -0.055 + 0.020 \frac{b}{c}$.

The following development of the unsteady viscous drag forces on a cable fairing segment using Whicker's loading functions could be applied to other loading functions as well. In the steady flow case the angle of inclination of the cable to the flow, θ, is identical to the trail angle, ϕ. The unsteady case is more complicated. First, the assumption is made that the drag coefficient for the steady flow applies to the unsteady case. Second, the local inflow velocity will depend on unsteady as well as steady terms, similarly the

angle of inclination of the fairing to the flow will involve more than the trail angle alone. Neglecting for the moment motion in the Z_o direction at any point along the cable the local flow will have components in the x_o, y_o coordinate system $U_o + \hat{u}_o$, $\hat{v}_o$. The magnitude of the inflow will then be $|V| = \sqrt{U_o^2 + 2U_o\hat{u}_o + \hat{u}_o^2 + \hat{v}_o^2}$. Then as shown in figure I-3 the angle of inclination to the flow θ will be given by

$$\theta = \phi - \beta \tag{I-6}$$

where $\beta = \hat{v}_o/U_o$ and $\phi = \phi^* + \hat{\phi}$. Furthermore the coordinate transformation from x_o, y_o, to x, y will give the local flow velocities in the cable coordinate system. They are

$$u = u^* + \hat{u} = (\sin\phi^* + \cos\phi^*\hat{\phi})(U_o+\hat{u}_o) - \cos\phi^*\hat{v}_o \tag{I-7a}$$

$$v = v^* + \hat{v} = (\cos\phi^* - \sin\phi^*\hat{\phi})(U_o+\hat{u}_o) + \sin\phi^*\hat{v}_o \tag{I-7b}$$

Equations (I-7a) and (I-7b) give

$$\hat{u}_o = \sin\phi^*\hat{u} + \cos\phi^*\hat{v} \tag{I-8a}$$

$$\hat{v}_o = -\cos\phi^*\hat{u} + \sin\phi^*\hat{v} + U_o\hat{\phi} \tag{I-8b}$$

Combining equations (I-8a,b), (I-6), (I-5a,b), (I-4a,b) and (I-3) will give expressions for the normal and tangential drag forces in terms of the dependent variables of the cable dynamics formulation.

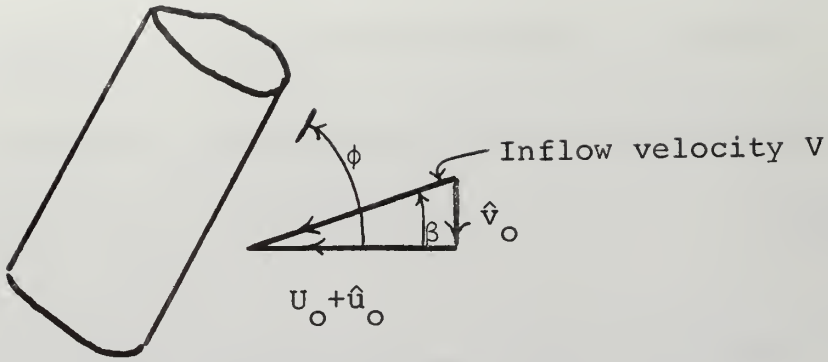

Figure I-3

Inflow Velocity and Components

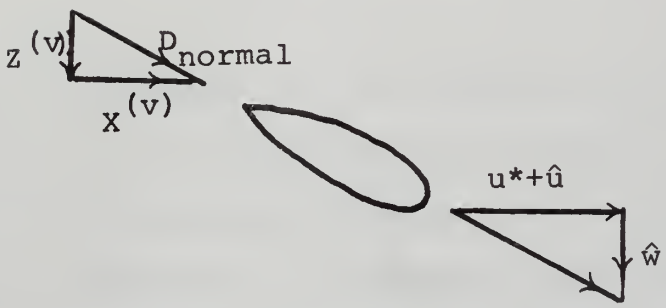

Figure I-4

Lateral Velocity and Force Diagram

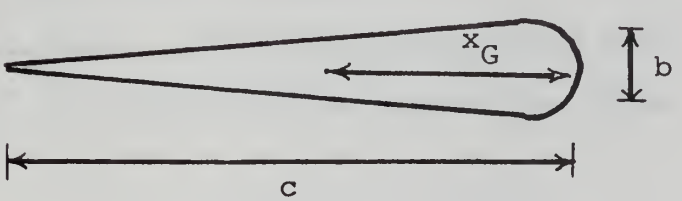

Figure I-5

Fairing Dimensions

$$D_{normal} = -C_D \tfrac{1}{2}\rho c\, ds[\{a_1+a_2\sin\phi^*\}\sin\phi^* U_o^2+\{(a_1+a_2\sin\phi^*) 2\sin^2\phi^*+(a_1+2a_2\sin\phi^*)\cos^2\phi^*\}U_o\hat{u}+a_1\sin\phi^*\cos\phi^* U_o\hat{v}] \quad \text{(I-9a)}$$

$$D_{tangential} = -C_D \tfrac{1}{2}\rho\, c\, ds[\{b_1+b_2\cos\phi^*\}\cos\phi^* U_o^2+b_1\sin\phi^* \cos\phi^* U_o\hat{u} + \{2(b_1+b_2\cos\phi^*)\cos^2\phi^* + (b_1+2b_2\cos\phi^*)\sin^2\phi^*\}U_o\hat{v}] \quad \text{(I-9b)}$$

Now that an expression for the normal force has been developed the effect of the z direction motion may be included. As shown in figure I-4 the normal component of the viscous drag on the fairing has components in both the x and z directions of the cable coordinate system. The z component results from the small component of velocity in the z direction, $\hat{w}$. The normal force is along the direction of the normal velocity, therefore it will have a z component proportional to the z direction velocity component. Similarly the x direction component of the normal force will be proportional to the x direction velocity component. Retaining only terms which are steady or linear in the perturbation quantities gives

$$Z^{(v)} = -C_D\, \tfrac{1}{2}\rho\, c\, ds\{a_1+a_2\sin\phi^*\}U_o\hat{w} \quad \text{(I-10a)}$$

$$X^{(v)} = -C_D \tfrac{1}{2}\rho\, c\, ds[\{a_1+a_2\sin\phi^*\}\sin\phi^* U_o^2 +$$

$$\{(a_1+a_2\sin\phi^*)2\sin^2\phi^* + (a_1+2a_2\sin\phi^*)\cos^2\phi^*\}$$

$$U_o\hat{u} + a_1\sin\phi^*\cos\phi^* U_o\hat{v}] \qquad \text{(I-10b)}$$

The component of the viscous force in the y direction is just the tangential force of equation (I-9b).

Thin Wing Theory

An effect of the flow about the fairing in the x-z plane is to develop a side force and moment on the fairing due to its behavior as a hydrofoil. The fairing is assumed to be a thin symmetrical foil moving approximately along its x axis with velocity u* but having also a small amplitude motion in the lateral or z direction. The resulting flow is assumed to be unaffected by the spanwise flow in the y direction. The results presented by Robinson and Laurmann (1952) for the two-dimensional motion of a thin wing with constant forward speed then apply to the fairing. These results include added mass and vortex effects. The equations for the hydrodynamic derivatives per unit length are

$$Z = Z_w \hat{w} + Z_{\dot{w}} \dot{\hat{w}} + Z_\alpha \hat{\alpha} + Z_q \hat{q} + Z_{\dot{q}} \dot{\hat{q}}$$

(I-11a,b)

$$M = M_w \hat{w} + M_{\dot{w}} \dot{\hat{w}} + M_\alpha \hat{\alpha} + M_q \hat{q} + M_{\dot{q}} \dot{\hat{q}}$$

where α is the fairing rotation angle and $q = \frac{\partial \alpha}{\partial t}$. Corrections must now be supplied for the thickness of the fairing and for the effect of rotations about the x and z axes with velocities $\hat{p}$ and $\hat{r}$. Examination of equations (I-2c) and (I-2e) show the presence of a term involving $X_{\dot{u}}$. This term is interpreted as a correction for thickness. Equations (I-2c) and (-2e) show no added mass effects proportional to $\hat{p}$ or $\hat{r}$, so the only contribution from these rotations could be from vortex effects. Such contributions are assumed to be of higher than first order in perturbation variables and are therefore not considered.

When considering the interaction of cable motion with the cable fairing the usual assumption (cf. Whicker (1957)) is that the fairing instantaneously aligns with the local direction of flow. In fact, of course, the fairing must respond to the dynamic interaction of the hydrodynamic forces from thin wing theory, thickness effects, and viscous drag with gravitational, inertial and external forces, the external force being the lateral force of contact between the cable and the fairing. The dynamic equations for the side force and moment per unit length acting on a fairing segment may now be written with the parameters of the lateral motion $\hat{\alpha}$, $\hat{w}$, and $\hat{\psi}$ as dependent variables. The equilibrium of forces gives

$$-m[\dot{\hat{w}}+\hat{p}v^*-\hat{q}u^*-x_G\dot{\hat{q}}]+(m-\rho V)g(\hat{\alpha}\cos\phi^*+\hat{\psi}\sin\phi^*)+Z^{(v)}+Z_w\hat{w}+Z_{\dot{w}}\dot{\hat{w}}+$$

$$Z_\alpha\hat{\alpha}+Z_q\hat{q}+Z_{\dot{q}}\dot{\hat{q}}-X_{\dot{u}}u^*\hat{q}+Z_c = 0 \qquad \text{(I-12)}$$

where m is the mass per unit length of fairing, V is the volume per unit length of fairing, x_G is the x distance from the origin to the center of gravity of the fairing, $Z^{(v)}$ is the viscous drag force of equation (I-10e) per unit length of fairing segment. Z_c is the force on the fairing from the cable and $\hat{p} = \frac{\partial \hat{\Psi}}{\partial t}$. Since it is more convenient to consider the mass of cable and fairing together in the parent problem, those terms of equation (I-11) which will appear directly in the inertial and gravitational force terms of the parent problem may be lumped in with the cable external force and (I-11) re-written as

$$Z_c = Z_w\hat{w} + Z_{\dot{w}}\dot{\hat{w}} + (Z_\alpha+(m-\rho V)g\cos\phi^*)\hat{\alpha} + (Z_q+mu^*-X_{\dot{u}}u^*)\hat{q} + (Z_{\dot{q}}+mx_G)\dot{\hat{q}} + Z^{(v)} \qquad \text{(I-13)}$$

Moment equilibrium gives

$$-I_y\dot{\hat{q}}+mx_G(\dot{\hat{w}}+\hat{p}v^*-\hat{q}u^*)+(m-\rho V)gx_G(\hat{\alpha}\cos\phi^*+\hat{\Psi}\sin\phi^*)+M_w\hat{w}+M_{\dot{w}}\dot{\hat{w}}+ M_\alpha\hat{\alpha}+M_q\hat{q}+M_{\dot{q}}\dot{\hat{q}}+X_{\dot{u}}u^*\hat{w}+Z^{(v)}x_p = 0 \qquad \text{(I-14)}$$

Where I_y is the mass moment of inertia per unit length of the fairing about the y axis, and x_p is the x distance from the origin to the point at which the resultant viscous drag force acts, a point near the leading edge of the fairing so x_p will be small compared to the chord c. Equation (I-14) may be rearranged to give

$$(-C_D\tfrac{1}{2}\rho c x_p(a_1+a_2\sin\phi^*)U_o+M_w+X_u\dot{}u^*)\hat{w}+(M_w\dot{}+mx_G)\dot{\hat{w}}+mx_G v^*\hat{p}+$$

$$(m-\rho V)gx_G\hat{\Psi}\sin\phi^* = -(M_\alpha+(m-\rho V)gx_G\cos\phi^*)\hat{\alpha}-(M_q-mx_G u^*)\hat{q}-$$

$$(M_q\dot{}-I_y)\dot{\hat{q}} \qquad \text{(I-15)}$$

Equation (I-15) may now be solved for $\hat{\alpha}$ as a function of $\hat{\Psi}$ and $\hat{w}$ and substituted back into equation (I-13) giving finally Z_c in terms of $\hat{\Psi}$ and $\hat{w}$. In view of the fact that the solution technique of the parent problem assumes solutions sinusoidal in time and that the hydrodynamic derivatives of equations (I-11a,b) are functions of frequency, equations (I-13) and (I-15) may be solved by assuming sinusoidal solutions in time. Suppose solutions are of the forms

$$\hat{w} = \bar{w}\, e^{i\omega t}$$

$$\hat{\alpha} = \bar{\alpha}\, e^{i\omega t}$$

$$\hat{\Psi} = \bar{\psi}\, e^{i\omega t}$$

$$Z_c = \bar{Z}_c e^{i\omega t}$$

Now substituting these solutions into equations (I-13) and (I-15) along with the values for the hydrodynamic derivatives given by Robinson and Laurmann (1952) leads to

$$\bar{Z}_c = [-(1-\tfrac{1}{2}H(\lambda))\pi\rho u^* c+(\tfrac{1}{2}G(\lambda)-\tfrac{1}{4})\pi\rho c^2 i\omega-C_D\tfrac{1}{2}\rho c(a_1+a_2\sin\phi^*)U_o]$$

$$\bar{w}+[-(1-\tfrac{1}{2}H(\lambda))\pi\rho u^{*2}c+(m-\rho V)g\cos\phi^*+((-1+\tfrac{3}{8}H(\lambda)+\tfrac{1}{2}G(\lambda))$$

$$\pi\rho u^* c^2+mu^*+\tfrac{1}{4}\pi\rho b^2 u^*)i\omega-((-\tfrac{1}{8}+\tfrac{3}{8}G(\lambda))\pi\rho c^3+mx_G)\omega^2]\bar{\alpha} \qquad \text{(I-16)}$$

$$[-C_D\tfrac{1}{2}\rho c x_p(a_1+a_2\sin\phi^*)U_o-\tfrac{1}{4}(1-\tfrac{1}{2}H(\lambda))\pi\rho u^*c^2-\tfrac{1}{4}\pi\rho b^2u^*+$$

$$((-\tfrac{1}{8}+\tfrac{1}{8}G(\lambda))\pi\rho c^3+mx_G)i\omega]\bar{w}+[mx_Gv^*i\omega+(m-\rho V)gx_G\sin\phi^*]\bar{\psi}= \qquad (I\text{-}17)$$

$$[-(-\tfrac{1}{4}(1-\tfrac{1}{2}H(\lambda))\pi\rho u^{*2}c^2+(m-\rho V)gx_G\cos\phi^*)-((\tfrac{3}{4}(-\tfrac{1}{2}+\tfrac{1}{8}H(\lambda)) +$$

$$\tfrac{1}{8}G(\lambda))\pi\rho u^*c^3-mx_Gu^*)i\omega+((-\tfrac{3}{128}-\tfrac{3}{16}(\tfrac{1}{4}-\tfrac{1}{2}G(\lambda))\pi\rho c^4-I_y)\omega^2]\bar{\alpha}$$

where $G(\lambda)$ and $H(\lambda)$ are given in terms of Bessel functions of the first and second kinds, that is Jn's and Yn's, as

$$H(\lambda) = 2\,\frac{J_o^2+Y_o^2+Y_oJ_1-J_oY_1}{(J_o-Y_1)^2+(J_1-Y_o)^2}, \qquad G(\lambda) = \frac{2}{\lambda}\,\frac{J_oJ_1+Y_oY_1}{(J_o-Y_1)^2+(J_1-Y_o)^2}$$

where λ the reduced frequency is given by $\lambda = \frac{\omega c}{u^*}$ and the argument of the Bessel functions is $\lambda/2$. We bear in mind that the inertial forces lumped into $\bar{Z}_c$ are of $0(\omega)$.

Equations (I-16) and (I-17) are rather complicated, but may be greatly simplified by placing some restrictions on the cable fairings and the conditions under which they are towed. First assume that the reduced frequency λ is such that $\lambda<<1$. This is justified by supposing that the driving frequency for lateral motion is the yaw frequency of the towing ship. Then typically $\omega\approx 1$ radian per sec. as determined from data presented in Korwin-Kroukowsky (1961). Typical fairings usually have a chord length less than 1 foot, so for velocities above several feet per sec. $\lambda<<1$. Second, real fairings are usually made of materials whose density is close to that of sea water so that gravity forces are very small, that is $m-\rho V\approx 0$. With little error the fairing geometry may be approximated as

shown in figure I-4. m, I_y, b and x_G may be replaced with expressions involving ρ and c, using the assumption that $m-\rho V=0$.

Equations (I-16) and (I-17) may be greatly simplified by eliminating inertial, gravitational and thickness effects. Assuming low reduced frequency allows us to replace G and H by the functions of λ to which they tend at low reduced frequency. With the above simplifications a surprising result follows. The side force on the cable contributed by the hydrodynamics of fairing acting as a thin wing at low reduced frequency, completely free to rotate about an axis through its leading edge is given by the classical added mass for a flat plate of the same span accelerating normal to its plane. To this may be added an inertial contribution proportional to the rate of change of the kiting angle arising from the center of gravity of the fairing not lying at the axis of the coordinate system, and the lateral component of viscous drag given in equation (I-10a).

To elucidate the fairing hydrodynamics the thin wing theory may be applied to the case of a massless flat plate to which the fairing has been reduced proceeding in the x direction with velocity u* being driven in harmonic oscillations normal to its line of travel by a force applied at its leading edge. The plate is free to rotate about its leading edge which is the y axis of a right-handed coordinate system. Equations for the forces and moments on the plate are

$$Z_{\dot{z}}\dot{z} + Z_{\ddot{z}}\ddot{z} + Z_{\alpha}\alpha + Z_{\dot{\alpha}}\dot{\alpha} + Z_{\ddot{\alpha}}\ddot{\alpha} = f_{ex} \qquad \text{(I-18)}$$

$$M_{\dot{z}}\dot{z} + M_{\ddot{z}}\ddot{z} + M_{\alpha}\alpha + M_{\dot{\alpha}}\dot{\alpha} + M_{\ddot{\alpha}}\ddot{\alpha} = 0 \qquad \text{(I-19)}$$

As before $z = z_o e^{i\omega t}$, $\alpha = \alpha_o e^{i\omega t}$ and $f_{ex} = f_o e^{i\omega t}$. Substituting into (I-18) and (I-19) the appropriate expressions for the hydrodynamic derivatives from Robinson and Laurmann (1952) gives

$$-(1-\tfrac{1}{2}H)\pi\rho u^* c i\omega z_o - (\tfrac{1}{2}G-\tfrac{1}{4})\pi\rho c^2\omega^2 z_o - (1-\tfrac{1}{2}H)\pi\rho u^{*2} c\alpha_o +$$

$$(-1+\tfrac{3}{8}H+\tfrac{1}{2}G)\pi\rho u^* c^2 i\omega\alpha_o + (\tfrac{1}{8}-\tfrac{3}{8}G)\pi\rho c^3\omega^2\alpha_o = f_o \qquad \text{(I-20)}$$

$$-\tfrac{1}{4}(1-\tfrac{1}{2}H)\pi\rho u^* c^2 i\omega z_o + (\tfrac{1}{8}-\tfrac{1}{8}G)\pi\rho c^3\omega^2 z_o - \tfrac{1}{4}(1-\tfrac{1}{2}H)\pi\rho u^{*2} c^2\alpha_o +$$

$$(-\tfrac{3}{8}+\tfrac{3}{32}H+\tfrac{1}{8}G)\pi\rho u^* c^3 i\omega\alpha_o - (-\tfrac{9}{128}+\tfrac{3}{32}G)\pi\rho c^4\omega^2\alpha_o = 0 \qquad \text{(I-21)}$$

Equation (I-21) may be solved for α_o giving

$$\alpha_o = \frac{-[i(-\tfrac{1}{4}+\tfrac{1}{8}H)+(\tfrac{1}{8}-\tfrac{1}{8}G)\lambda]\frac{\lambda z_o}{c}}{[(-\tfrac{1}{4}+\tfrac{1}{8}H)+i(-\tfrac{3}{8}+\tfrac{3}{32}H+\tfrac{1}{8}G)\lambda+(\tfrac{9}{128}-\tfrac{3}{32}G)\lambda^2]} \qquad \text{(I-22)}$$

where $\frac{\omega c}{u^*} = \lambda$

similarly equation (I-20) may be rewritten as

$$[-i(1-\tfrac{1}{2}H)-(\tfrac{1}{2}G-\tfrac{1}{4})\lambda]\frac{\lambda z_o}{c} + [-(1-\tfrac{1}{2}H)+(-1+\tfrac{3}{8}H+\tfrac{1}{2}G)i\lambda +$$

$$(\tfrac{1}{8}-\tfrac{3}{8}G)\lambda^2]\alpha_o = \frac{f_o}{\pi\rho u^{*2} c} \qquad \text{(I-23)}$$

and substituting into (I-23) from (I-22) gives

$$\{-[i(1-\tfrac{H}{2})+(\tfrac{G}{2}-\tfrac{1}{4})\lambda]+A(\lambda)[i(1-\tfrac{H}{2})+(\tfrac{G}{2}-\tfrac{1}{2})\lambda]\lambda\}\frac{z_o}{c} = \frac{f_o}{\pi\rho u^{*2}c} \qquad \text{(I-24)}$$

where $A(\lambda) = \dfrac{[(-1+\frac{1}{2}H)+(-1+\frac{3}{8}H+\frac{1}{2}G)i\lambda+(\frac{1}{8}-\frac{3}{8}G)\lambda^2]}{[(-1+\frac{1}{2}H)+(-\frac{3}{2}+\frac{3}{8}H+\frac{1}{2}G)i\lambda+(\frac{9}{32}-\frac{3}{8}G)\lambda^2]}$

$H(\lambda)$, $G(\lambda)$, and $A(\lambda)$ must now be evaluated for low reduced frequency. This is done by looking at series for the Bessel functions J_o, J_1, Y_o, Y_1 for small values of their arguments. From Jahnke and Emde (1945)

$$J_o(\lambda/2) = 1 - \frac{\lambda^2}{16} + 0(\lambda^4)$$

$$J_1(\lambda/2) = \frac{\lambda}{4} + 0(\lambda^3)$$

$$Y_o(\lambda/2) = \frac{2}{\pi}[\ln\frac{\gamma\lambda}{4} - \frac{\lambda^2}{16}\ln\frac{\gamma\lambda}{4} + \frac{\lambda^2}{16} + 0(\lambda^4 \ln\lambda)]$$

$$Y_1(\lambda/2) = \frac{1}{\pi}[-\frac{4}{\lambda} + \frac{\lambda}{2}\ln\frac{\gamma\lambda}{4} - \frac{\lambda}{4} + 0(\lambda^3\ln\lambda)]$$

where $\gamma = 1.781$. Substituting these relationships into the expressions for G and H leads to

$$H = \frac{\pi\lambda}{2} + \frac{\lambda^2}{2}\ln^2\frac{\gamma\lambda}{4} - \frac{3\pi^2\lambda^2}{16} + 0(\lambda^3\ln^2\lambda)$$

$$G = -\ln\frac{\gamma\lambda}{4} + \frac{\pi\lambda}{2}\ln\frac{\gamma\lambda}{4} + 0(\lambda^2\ln^3\lambda)$$

Substituting these expressions into the expression for $A(\lambda)$ gives

$$A(\lambda) = 1 - \frac{i\lambda}{2} + 0(\lambda^2 \ln^2 \lambda) \qquad \text{(I-25)}$$

Now putting $A(\lambda)$, $G(\lambda)$, and $H(\lambda)$ into equation (I-24) gives

$$\left(\frac{\lambda}{4} + 0(\lambda^2 \ln^2 \lambda)\right) \lambda \frac{z_o}{c} = \frac{f_o}{\pi \rho u^{*2} c}$$

or

$$f_o = -\tfrac{1}{4}\pi \rho c^2 (i\omega)^2 \, z_o. \qquad \text{(I-26)}$$

Noticing that $i\omega$ indicates differentiation with respect to time, the results of equation (I-26) combined with (I-10a) and the term proportional to $\frac{\partial \psi}{\partial t}$ caused by the center of gravity of the fairing not being on the coordinate axis give

$$Z_c = -\tfrac{1}{4}\pi \rho c^2 \frac{\partial \hat{w}}{\partial t} - \frac{4mx_G}{c} v^* \frac{\partial \hat{\psi}}{\partial t} - C_D \tfrac{1}{2}\rho c (a_1 + a_2 \sin\phi^*) U_o \hat{w} \qquad \text{(I-27)}$$

Then the lateral hydrodynamic force on a segment of fairing of length ds is

$$Z^{(h)} = -\tfrac{1}{2}\rho C_D c ds (a_1 + a_2 \sin\phi^*) U_o \hat{w} - \tfrac{1}{4}\pi \rho c^2 ds \frac{\partial \hat{w}}{\partial t} - \frac{4mx_G}{c} v^* ds \frac{\partial \hat{\psi}}{\partial t} \qquad \text{(I-28)}$$

Results

The total hydrodynamic force acting on the cable in the x direction may be written by combining equations (I-2a) and (I-10b) giving

$$X^{(h)} = -\tfrac{1}{4}\rho\pi b^2 ds \frac{\partial \hat{u}}{\partial t} - C_D \tfrac{1}{2}\rho cds[\{a_1+a_2\sin\phi^*\}\sin\phi^* U_o^2 + \{(a_1+a_2\sin\phi^*)2\sin^2\phi^*+(a_1+2a_2\sin\phi^*)\cos^2\phi^*\}U_o\hat{u} + a_1\sin\phi^*\cos\phi^* U_o\hat{v}] \quad \text{(I-29)}$$

Similarly the total hydrodynamic force acting on the cable in the y direction is given by combining equations (I-2b) and (I-9b)

$$Y^{(h)} = -\tfrac{1}{4}\rho\pi b^2 ds\, u^* \frac{\partial \hat{\phi}}{\partial t} - C_D \tfrac{1}{2}\rho cds[\{b_1+b_2\cos\phi^*\}\cos\phi^* U_o^2 + b_1\sin\phi^*\cos\phi^* U_o\hat{u} + \{2(b_1+b_2\cos\phi^*)\cos^2\phi^* + (b_1+2b_2\cos\phi^*)\sin^2\phi^*\}U_o\hat{v}] \quad \text{(I-30)}$$

and finally the total hydrodynamic force on the cable in the lateral direction is given by equation (I-28).

The above results of the compound hydrodynamic theory of the three dimensional unsteady motions of a cable fairing segment leave much to be desired in three areas. First the theory is more a collection of results bound together by assumption than a single cohesive formulation. Second, it lacks experimental evidence by which to test its validity. Third, the case for the non-neutrally buoyant fairing with inertial and thickness effects retained as in equations (I-16)

and (I-17) needs to be worked out. The usefulness of the theory in the absence of a more comprehensive one is that it provides a basis from which to attack the parent problem.

Appendix II

HYDRODYNAMICS OF THE TOWED BODY

The body under tow in this thesis is a sphere towed from its center of gravity and buoyancy. This is, of course, the simplest possible towed body and provides the simplest dynamic boundary condition at the end of the cable. Real towed bodies are often quite complicated, employing fairings to reduce drag, depressors to promote deeper towing, and control surfaces to alter local orientation, and in very advanced systems, propulsion. These latter bodies may impose very complicated boundary conditions on the cable.

The equations of motion of the sphere derive from considering the inertial forces of its mass and added mass, its weight, and its drag all balanced by the tension in the cable. Components of the inertial forces in the respective coordinate directions are

$$F_x^{(i)} = -(M_B + \mu_B)\left(\frac{\partial \hat{u}}{\partial t} - v^* \frac{\partial \hat{\phi}}{\partial t}\right)$$

$$F_y^{(i)} = -(M_B + \mu_B)\left(\frac{\partial \hat{v}}{\partial t} + u^* \frac{\partial \hat{\phi}}{\partial t}\right) \qquad \text{(II-1)}$$

$$F_z^{(i)} = -(M_B + \mu_B)\left(\frac{\partial \hat{w}}{\partial t} + v^* \frac{\partial \hat{\psi}}{\partial t}\right)$$

where M_B is the mass of the body and μ_B is the added mass which for a deeply submerged sphere is 1/2 the displacement.

Gravitational forces are

$$F_x^{(g)} = (M_B - \rho\forall_B)\, g(\cos\phi^* - \sin\phi^*\hat{\phi})$$

$$F_y^{(g)} = -(M_B - \rho\forall_B)\, g(\sin\phi^* + \cos\phi^*\hat{\phi}) \qquad \text{(II-2)}$$

$$F_z^{(g)} = (M_B - \rho\forall_B)\, g \sin\phi^*\hat{\Phi}$$

where $\forall_B$ is the volume of the sphere and ρ the density of the water.

Drag forces are found by considering the sphere to be moving through the water with velocity $\vec{W}$. The drag is then given by $\vec{F}^{(d)} = -\frac{1}{2}\rho C_T\, S|W|\vec{W}$ where C_T is a drag coefficient which is a function of Reynold's number and A_B is the frontal area of the sphere. But

$$|W| = \sqrt{u^{*2} + v^{*2}}\ \left(1 + \frac{u^*\hat{u}}{u^{*2}+v^{*2}} + \frac{v^*\hat{v}}{u^{*2}+v^{*2}}\right)$$

retaining only the steady terms and the terms linear in the perturbation velocities. Drag force components are

$$F_x^{(d)} = -\tfrac{1}{2}\rho C_T\, A_B\, |W|\ \ (u^* + \hat{u})$$

$$F_y^{(d)} = -\tfrac{1}{2}\rho C_T\, A_B\, |W|\ \ (v^* + \hat{v}) \qquad \text{(II-3)}$$

$$F_z^{(d)} = -\tfrac{1}{2}\rho C_T\, A_B\, |W|\ \ \hat{w}$$

And finally

$$F_x^{(d)} = -\tfrac{1}{2}\rho C_T A_B U_o^2 \left(\frac{u^*}{U_o} + \frac{\hat{u}}{U_o} + \frac{u^{*2}\hat{u}}{U_o^3} + \frac{u^*v^*\hat{v}}{U_o^3}\right)$$

$$F_y^{(d)} = -\tfrac{1}{2}\rho C_T A_B U_o^2 \left(\frac{v^*}{U_o} + \frac{\hat{v}}{U_o} + \frac{v^{*2}\hat{v}}{U_o^3} + \frac{v^*u^*\hat{u}}{U_o^3}\right) \qquad \text{(II-4)}$$

$$F_z^{(d)} = -\tfrac{1}{2}\rho C_T A_B U_o \hat{w}$$

where $U_o = \sqrt{u^{*2} + v^{*2}}$

Tension acts only in the y direction along the cable and is given by

$$F^{(T)} = T^* + \hat{T} \qquad \text{(II-5)}$$

Combining equations (II-1, 2, 4, 5) gives the equations of motion for a towed sphere.

$$-(M_B+\mu_B)\left(\frac{\partial\hat{u}}{\partial t} - v^*\frac{\partial\hat{\phi}}{\partial t}\right) - \tfrac{1}{2}\rho C_T A_B U_o^2 \left(\frac{u^*}{U_o} + \frac{\hat{u}}{U_o} + \frac{(u^{*2}\hat{u}+u^*v^*\hat{v})}{U_o^3}\right) +$$

$$(M_B-\rho\forall_B)\, g(\cos\phi^* - \sin\phi^*\hat{\phi}) + f_x = 0$$

$$-(M_B+\mu_B)\left(\frac{\partial\hat{v}}{\partial t} + u^*\frac{\partial\hat{\phi}}{\partial t}\right) - \tfrac{1}{2}\rho C_T A_B U_o^2 \left(\frac{v^*}{U_o} + \frac{\hat{v}}{U_o} + \frac{(v^{*2}\hat{v}+v^*u^*\hat{u})}{U_o^3}\right)$$

$$-(M_B-\rho\forall_B)\, g(\sin\phi^* + \cos\phi^*\hat{\phi}) + T^* + \hat{T} + f_y = 0$$

$$-(M_B+\mu_B)\left(\frac{\partial\hat{w}}{\partial t} + v^*\frac{\partial\hat{\psi}}{\partial t}\right) + (M_B-\rho\forall_B)\, g\,\hat{\psi}\sin\phi^* - \tfrac{1}{2}\rho C_T A_B U_o \hat{w} + f_z = 0$$

(II-6)

In these euqations f_x, f_y and f_z are included as the source of possible perturbing forces such as might be created by body control mechanisms. For the simplest case these vanish.

Considering a general body towed at some arbitrary point vice a sphere towed at its center of gravity and buoyancy complicates matters. Moments must be considered in writing the equations of motion of the body and method of attachment of the body to the tow cable becomes a matter of critical interest. Eames (1966) considered the general problem in some detail.

Appendix III

SPECIAL CASES

The elements of the coefficient matrix of the cable equations of motion are constant for certain special cases. Solutions can then be constructed from the eigenvalues and eigenvectors of the coefficient matrix. Two cases are considered. In one case the cable is neutrally buoyant and has no viscous drag. The cable tows in a straight line at whatever trail angle is specified by the towed body weight and drag. As before, the lateral motions may be considered separately from the transverse-longitudinal motions. In a second case the cable and the towed body are neutrally buoyant. Normal viscous drag acts on the cable but no tangential drag. The trail angle is zero, that is the body tows directly astern of the tow point. In this case lateral motions, transverse motions and longitudinal motions are all decoupled and the lateral and transverse modes are identical in form differing only in the value of cable added mass. The point is to show that the results obtained from these special cases by a simple analysis agree with the results obtained from the general formulation and analysis when specialized for the same cases.

As mentioned before in Chapter 3 when the coefficient matrix is constant solutions are obtained as follows

$$\frac{d\bar{x}}{d\zeta} = [a]\ \bar{x} \qquad \text{(III-1)}$$

where $\bar{x}$ is the appropriate vector of n dependent variables and [a] is an n x n coefficient matrix.

$$|a-\lambda I| = 0 \qquad \text{(III-2)}$$

gives n eigenvalues of [a].

$$[a]\bar{c}_i = \lambda_i \bar{c}_i \qquad \text{(III-3)}$$

gives i^{th} eigenvector of [a] associated with i^{th} eigenvalue.

$$\bar{x} = \sum_{i}^{n} \bar{c}_i \, e^{\lambda i \zeta} \qquad \text{(III-4)}$$

gives the solution in terms of the arbitrary constants of the $\bar{c}_i$. Boundary conditions provide n equations in the n arbitrary constants when the equations (III-4) are substituted into them for the values of the dependent variables. Solution of these equations gives the values of the n arbitrary constants, which are substituted back into (III-4) giving the final form of the solution.

The equations of motion are first written in their complex normal forms and specialized for the particular case at hand. The above steps are accomplished. The results are transformed into the local vertical coordinate system and the motions at the towed body are compared with those given by the general formulation, method and program. In all cases the comparison shows agreement. Even for these simple cases the algebra and the computation of the results is tedious so simple arithmetic programs were written to do this work.

Neutrally Buoyant Cable Without Drag

Lateral Motions

The equations of motion are

$$\begin{pmatrix} \frac{dw}{d\zeta} \\ \\ \frac{d\psi}{d\zeta} \end{pmatrix} = \begin{pmatrix} -i\nu\frac{(1+\eta)}{N}\cos\Phi & -i\nu\left(\frac{\cos^2\Phi}{N} - \frac{1}{\delta}\right) \\ \\ \frac{i\nu(1+\eta)}{N} & \frac{i\nu\cos\Phi}{N} \end{pmatrix} \begin{pmatrix} w \\ \\ \psi \end{pmatrix} \qquad \text{(III-5)}$$

with $d = 1$, $D = 0$, $h = 0$, $\gamma \to \infty$.

The steady configuration equations give

$$\frac{d\Phi}{d\zeta} = 0, \quad \frac{dN}{d\zeta} = 0, \quad N = C\sqrt{1+\tan^2\Phi}, \quad \Phi = \Phi_c = \tan^{-1}\left(\frac{M-a}{C}\right) \qquad \text{(III-6)}$$

The boundary conditions are

$$\begin{aligned} \zeta = 0 \quad & (i\nu(M+k)+C)w + (i\nu(M+k)\cos\Phi-(M-a)\sin\Phi)\psi = 0 \\ \zeta = 1 \quad & w + \cos\Phi\,\psi = \varepsilon \end{aligned} \qquad \text{(III-7)}$$

The eigenvalues are

$$\lambda_{\frac{1}{2}} = f \pm g$$

$$f = -i\nu p; \quad g = i\nu\sqrt{p^2+q^2}$$

$$p = \frac{\cos\Phi\eta}{2N}; \quad q = \sqrt{\frac{(1+\eta)}{N\delta}}$$

Recalling that $w_o = w + \cos\Phi\psi$ we may, after some algebra, write

$$w_o = \varepsilon e^{-i\nu p(\zeta-1)} \quad \frac{(-[(\cos\Phi p+\frac{1}{\delta})C+(M-a)\sin\Phi p]\sin(\nu\sqrt{p^2+q^2}\zeta)+}{(-[(\cos\Phi p+\frac{1}{\delta})C+(M-a)\sin\Phi p]\sin(\nu\sqrt{p^2+q^2}) +}$$

$$\frac{i[\frac{\sqrt{p^2+q^2}N^2\cos\Phi}{C}\cos(\nu\sqrt{p^2+q^2}\zeta)-\frac{\nu(M+k)}{\delta}\sin(\nu\sqrt{p^2+q^2}\zeta)])}{i[\frac{\sqrt{p^2+q^2}\ N^2\cos\Phi}{C}\cos(\nu\sqrt{p^2+q^2}) - \frac{\nu(M+k)}{\delta}\sin(\nu\sqrt{p^2+q^2}\ )])}$$

(III-8)

from which the magnitude of w_o at $\zeta = 0$ may readily be calculated. For a test cable with M= 3.0, a = 2.0, k = 1.0, δ = 0.01, ε_R = 1.0, ε_I = 0.0, c = 1.0, η = 1.0 agreement between the above formulas and the general program was exact to at least five significant digits for values of ν from 0.0 to 1.0.

Transverse-Longitudinal Motions

The equations of motion are

$$\begin{pmatrix} \frac{du}{d\zeta} \\ \frac{d\phi}{d\zeta} \\ \frac{dv}{d\zeta} \\ \frac{dn}{d\zeta} \end{pmatrix} = \begin{pmatrix} -\frac{i\nu\cos\Phi(1+\mu)}{N} & i\nu[\frac{\cos^2\Phi}{N} - \frac{1}{\delta}(1+\frac{N}{\gamma})] & 0 & 0 \\ -\frac{i\nu(1+\mu)}{N} & \frac{i\nu\cos\Phi}{N} & 0 & 0 \\ \frac{i\nu\sin\Phi(1+\mu)}{N} & -i\nu\sin\Phi\cos\Phi & 0 & \frac{i\nu}{\gamma\delta} \\ 0 & i\nu(1+\mu)\sin\Phi & i\nu & 0 \end{pmatrix} \begin{pmatrix} u \\ \phi \\ v \\ n \end{pmatrix}$$

(III-9)

The steady configuration equations are as above for lateral motions. The boundary conditions are

$$\zeta=0 \quad [i\nu(M+k)+C(1+\sin^2\Phi)]u+[-i\nu(M+k)\cos\Phi+(M-a)\sin\Phi]\phi +$$
$$C\sin\Phi\cos\Phi v = 0$$

$$C\sin\Phi\cos\Phi\, u + [i\nu(M+k)\sin\Phi+(M-a)\cos\Phi]\phi + \qquad \text{(III-10)}$$
$$[i\nu(M+k) + C(1+\cos^2\Phi)]v - n = 0$$

$$\zeta=1 \quad u-\cos\Phi\phi = \alpha = \sin\Phi\, \delta u - \cos\Phi\, he$$

$$v+\sin\Phi\phi = \beta = \cos\Phi\, \delta u + \sin\Phi\, he$$

The eigenvalues are

$$\lambda_{\frac{1}{2}} = \frac{i\nu\cos\Phi}{2N} \left(-\mu \pm \sqrt{\mu^2 + \frac{4(1+\mu)N(1+N/\gamma)}{\delta\cos^2\Phi}}\right) \qquad \text{(III-11)}$$

$$\lambda_{\frac{3}{4}} = \pm i\nu \sqrt{\frac{1}{\gamma\delta}}$$

The solutions are given by

$$\begin{pmatrix} u \\ \phi \\ v \\ n \end{pmatrix} = \begin{pmatrix} \alpha_1 \\ b_1\alpha_1 \\ c_1\alpha_1 \\ d_1\alpha_1 \end{pmatrix} e^{\lambda_1\zeta} + \begin{pmatrix} \alpha_2 \\ b_2\alpha_2 \\ c_2\alpha_2 \\ d_2\alpha_2 \end{pmatrix} e^{\lambda_2\zeta} + \begin{pmatrix} 0 \\ 0 \\ \alpha_3 \\ d_3\alpha_3 \end{pmatrix} e^{\lambda_3\zeta} + \begin{pmatrix} 0 \\ 0 \\ \alpha_4 \\ d_4\alpha_4 \end{pmatrix} e^{\lambda_4\zeta} \qquad \text{(III-12)}$$

where the b's, c's and d's are combinations of eigenvalues and coefficient matrix elements found by solving for the eigenvectors and the α's are the arbitrary constants of the eigenvectors found by substituting equations (III-12) into equations (III-10). The resulting algrbra is tedious so results were obtained by computer solutions from this point on. The magnitudes of u_o, v_o and n at ζ=0 were calculated and compared with results from the general program for the following cable. M=3.0, a=2.0, k=1.0, C=1.0, γ=100.0, δ=0.01, μ=1.0, δu_R=1.0, δu_I=0.0, he_R=1.0, he_I=0.0 with ν between 0.0 and 1.0. Results compared favorably through the third significant digit. The small remaining difference seems to be the result of the matrix inversion carried out in the special case solution where solving for the arbitrary constants of the eigenvectors by Cramer's Rule. The largest difference occurred near a reasonance condition at ν=0.3 and was less than 2%. Such a reasonance is to be expected since these cases have no damping except that which is introduced by the towed body boundary condition.

Neutrally Buoyant Cable and Body With Normal Drag

Lateral or Transverse Motions

The equations of motion are

$$\begin{pmatrix} \frac{dw}{d\zeta} \\ \\ \frac{d\psi}{d\zeta} \end{pmatrix} = \begin{pmatrix} -\frac{(i\nu(1+\eta)+D_7)}{N} & -i\nu\left(\frac{1}{N}-\frac{1}{\delta}\right) \\ \\ \frac{(i\nu(1+\eta)+D_7)}{N} & +\frac{i\nu}{N} \end{pmatrix} \begin{pmatrix} w \\ \\ \psi \end{pmatrix} \qquad \text{(III-13)}$$

with d=1, N=C, $b_1=b_2=0$, M=a and $\Phi=0$ so $\sin\Phi=0$ and $\cos\Phi=1$ and $\gamma=100.0$. Steady configuration of the cable is trailing dead astern. Boundary conditions are

$$\zeta = 0 \qquad (-i\nu(M+k)-C)w - i\nu(M+k)\psi = 0$$

$$\zeta = 1 \qquad w \qquad \psi = 0 \qquad \text{(III-14)}$$

The eigenvalues are

$$\lambda_{\frac{1}{2}} = f \pm g$$

$$f = \frac{-D_7}{2N} - \frac{i\nu\eta}{2N} \qquad \text{(III-15)}$$

$$g = \frac{1}{2N}\sqrt{D_7^2 - \nu^2(\eta^2 + \frac{4(1+\eta)N}{\delta}) + i2\nu D_7(\eta + \frac{2N}{\delta})}$$

Suppose we also define for convenience three more constants

$$A = \frac{CD_7}{2N} - \nu^2\frac{(M+k)}{\delta}$$

$$B = \nu C(\frac{\eta}{2N} + \frac{1}{\delta}) \qquad \text{(III-16)}$$

$$G = A + iB$$

now as in the first case above we may write

$$w_o = \varepsilon e^{f(\zeta-1)}\left\{\frac{G(e^{g\zeta}-e^{-g\zeta}) + gC(e^{g\zeta}+e^{-g\zeta})}{G(e^{g}-e^{-g}) + gC(e^{g}+e^{-g})}\right\} \qquad \text{(III-17)}$$

The magnitude of w_o at $\zeta=0$ may be calculated easily and compared with results for the general programs. Here as before the results are exactly similar through the fifth significant digit. The equations for the transverse motion are identical with η replaced by μ and w, ψ replaced by u, ϕ. The magnitude of v_o at $\zeta=0$ was calculated and again compared exactly with results from the general program through the fifth significant digit.

Longitudinal Motion

The equations of motion are

$$\begin{pmatrix} \frac{dv}{d\zeta} \\ \\ \frac{dn}{d\zeta} \end{pmatrix} = \begin{pmatrix} 0 & \frac{i\nu}{\gamma\delta} \\ \\ i\nu & 0 \end{pmatrix} \begin{pmatrix} v \\ \\ n \end{pmatrix} \qquad \text{(III-18)}$$

for same cable parameters as in the lateral or transverse case. The boundary conditions are

$$\zeta = 0 \qquad -i\nu(M+k)v - 2C\,v + n = 0$$

$$\zeta = 1 \qquad v = \beta = \delta u \qquad \text{(III-19)}$$

The eigenvalues are $\lambda_{\frac{1}{2}} = \pm\frac{i\nu}{\sqrt{\gamma\delta}}$ (III-20)

The solutions are

$$v = \delta u \frac{\left[\sqrt{\gamma\delta}\cos\left(\frac{\nu\zeta}{\sqrt{\gamma\delta}}\right) - \nu(M+k)\sin\left(\frac{\nu\zeta}{\sqrt{\gamma\delta}}\right) + 2iC\sin\left(\frac{\nu\zeta}{\sqrt{\gamma\delta}}\right)\right]}{\left[\sqrt{\gamma\delta}\cos\left(\frac{\nu}{\sqrt{\gamma\delta}}\right) - \nu(M+k)\sin\left(\frac{\nu}{\sqrt{\gamma\delta}}\right) + 2iC\sin\left(\frac{\nu}{\sqrt{\gamma\delta}}\right)\right]} \quad \text{(III-21)}$$

$$n = \delta u \frac{\left[\sqrt{\gamma\delta}\left[2C\cos\left(\frac{\nu\zeta}{\sqrt{\gamma\delta}}\right) + i\left(\sqrt{\gamma\delta}\sin\left(\frac{\nu\zeta}{\sqrt{\gamma\delta}}\right) + \nu(M+k)\cos\left(\frac{\nu\zeta}{\sqrt{\gamma\delta}}\right)\right)\right]\right]}{\left[\sqrt{\gamma\delta}\cos\left(\frac{\nu}{\sqrt{\gamma\delta}}\right) - \nu(M+k)\sin\left(\frac{\nu}{\sqrt{\gamma\delta}}\right) + 2iC\sin\left(\frac{\nu}{\sqrt{\gamma\delta}}\right)\right]} \quad \text{(III-22)}$$

From these solutions, as before, the magnitudes of u_o and n were calculated and compared to the result from the general program. Again agreement was exact through five significant digits.

The results of these special cases match closely the results of the general program lending credence to the numerical method employed.

Appendix IV

TRIAL CABLE

The basic towed cable system used in Chapter 4 was developed from the following specifications.

Tow cable: length-1200 ft., diameter-1/2 in., weight per foot of cable plus fairing-1/2 lb., material-steel with modulus of elasticity 20×10^6 psi[1]

Fairing: breadth-0.555 in., mean chord-2.22 in., drag coefficient-0.1[2]

Body: sphere-40 in. diameter, weight-2482 lbs., displacement-1241 lbs., drag coefficient-0.15[3]

Tow Speed: 16 feet per sec. (approximately 10 kts.)

Frequency range of excitation: Angular frequency - 0.0 to 1.0

The above specifications give the following cable and body parameters using the definitions of Chapter 2.

$d=0.125$ $\gamma=4160.0$ $M=4.14$ $C=0.56$ $a=2.07$ $D=9.48$ $\delta=0.0066$

$b=0.555$ $c=2.22$ $\mu=0.214$ $k=1.03$ $\eta=3.44$ $\xi=0.5$ $h=0.5$

---

(1) Meyers, Holm, McAllister, Handbook of Ocean and Underwater Engineering, New York, 1969.

(2) Fathom Oceanology Limited Brochure Describing the cable fairing called "Flexnose" distributed by Fathom Oceanology Limited, 863 Rangeview Road, Port Credit, Ontario.

(3) Hoerner, S.F., Fluid Dynamic Drag, Midland Park, New Jersey, 1965.

BIBLIOGRAPHY

This bibliography contains entries in two categories. First, books and articles which were used directly in the work of this thesis, and second, books and articles which are relevant to the area of cable dynamics but had no impact on this thesis. Casarella and Parsons compiled a very complete bibliography for their article "A Survey of Investigations and Motions of Cable Systems Under Hydrodynamic Loading" published in the Marine Technology Society Journal, vol. 4, no. 4 of July-August 1970. No entry in their bibliography is repeated here unless it belongs in the first category mentioned above.

Category I

Abkowitz, M.A., *The Stability of a Segment of a Faired Cable as Part of a Tethered System*, Joseph Kaye & Co., Inc., Report 68, October 1965.

Abkowitz, M.A., *The Stability of a Faired Cable of a Tethered System in its Fundamental Mode*, Joseph Kaye & Co., Inc., Report 73, September 1967.

Abkowitz, M.A., *Stability and Motion Control of Ocean Vehicles*, MIT Press, 1969.

Calkins, D.E., "Faired Towline Hydrodynamics", *Journal of Hydronautics*, Vol. 4, No. 3, July 1970.

Casarella, M.J. and Parsons, M., "A Survey of Investigations and Motions of Cable Systems Under Hydrodynamic Loading", *MTS Journal*, Vol. 4, No. 4, July-August 1970.

Choo, Y., *Analytical Investigation of the Three-Dimensional Motion of Towed Systems*, Catholic University of America Dissertation, University Microfilms 70-22,091, 1970.

Choo, Y. and Casarella, M.J., "Hydrodynamic Resistance of Towed Cables", *Journal of Hydronautics*, Vol. 5, No. 4, October 1971.

Cristescu, N., "Rapid Motions of Extensible Strings", *Journal of Mechanics and Physics of Solids*, Vol. 12, 1964.

Eames, M.C., *Initial Approach to Cable Influence on Longitudinal Towed-Body Dynamics*, NRE Technical Note FM/64/7, September, 1964.

Eames, M.C., *Summary of the Linear Equations of Motion and Stability Derivatives for Towed Bodies*, NRE Technical Note FM/66/2, February 1966.

Froidevaux, M.R., *Application of Statistical Estimation to The Determination of Ocean Current-Meter Dynamics*, MIT Instrumentation Laboratory Report, T-494, January 1968.

Hochstadt, H., *Differential Equations*, New York, 1964.

Hoerner, S.F., *Fluid-Dynamic Drag*, Midland Park, New Jersey, 1965.

Huffman, R.R., *The Dynamical Behavior of an Extensible Cable in a Uniform Flow Field (An Investigation of the Towed Vehicle Problem)*, Purdue University Dissertation, 1969.

Huffman, R.R. and Genin, J., "The Dynamical Behavior of a Flexible Cable in a Uniform Flow Field", *The Aeronautical Quarterly*, May 1971.

IBM System/360, *Scientific Subroutine Package*, Version III, Programmer's Manual, 1970.

Imlay, F.H., *The Complete Expressions for "Added Mass" of a Rigid Body Moving in an Ideal Fluid*, DTMB Report 1528, July 1961.

Jahnke, E. and Emde, F., *Tables of Functions*, 1945.

Kerney, K.P., *Small Perturbation Analysis of Oscillatory Tow-Cable Motion*, Naval Ship Research and Development Ship Performance Department Report 3430, November 1971.

Korwin-Kroukowsky, D.V., *Theory of Seakeeping*, 1961.

Milgram, J.H., "Forces and Motions of a Flexible Floating Barrier", *Journal of Hydronautics*, Vol. 5, No. 2, April 1971.

Morse, P.M., *Vibration and Sound*, New York, 1948.

Morse, P.M. and Feshbach, H., *Methods of Theoretical Physics*, New York, 1953.

Pode, L., *Tables for Computing the Equilibrium Configuration of a Flexible Cable in a Uniform Stream*, DTMB Report No. 687, March 1951.

Robinson, A. and Laurman, J.A., *Wing Theory*, 1952.

Schram, J.W. and Reyle, S.P., "A Three Dimensional Dynamic Analysis of a Towed System", *Journal of Hydronautics*, Vol. 2, No. 4, October 1968.

Timoshenko, S. and Young, D.H., *Vibration Problems in Engineering*, New York, 1955.

Volterra, E. and Zachmanoglou, E.C., *Dynamics of Vibrations*, Columbus, Ohio, 1965.

Whicker, L.F., *The Oscillatory Motion of Cable-Towed Bodies*, University of California Dissertation, 1957.

Category II

Boeing Co., Seattle Aerospace Group, *Development of High Speed Towing Cables/Underwater Towed Body*, Part II, Vol. II, Boeing Co. Seattle Aerospace Group (N123 (9521)52187a), U. S. Clearing House (AD804190), 1966.

Brainard, J.P., *Dynamic Analysis of a Single Point, Taut, Compound Mooring*, WHOI Report Reference No. 71-42, June 1971.

Brion, J.N., *Tests and Investigations of a High Speed Towed Sonar Cable*, Boeing Company Seattle Aerospace Group (N123(953)33813a), U. S. Clearing House (AD-443393), 1965.

Campbell, J.F., *Dynamics of Towed Decelerators*, Langley Research Center, Langley Station, Va., U. S. Clearing House (N6919898), 1968.

Casarella, M.J. and Laura, P.A., "Drag on an Oscillating Rod with Longitudinal and Torsional Motion, *Journal of Hydronautics*, Vol. 3, No. 4, 1969.

Dale, J.R., *Vortex Effects on Flexible Cables*, Proceedings Symposium on O.E. University of Pennsylvania, 1970.

Dominguez, R.F. and Filmer, R.W., *Discrete Parameter Analysis as a Practical Means for Solving Mooring Behavior Problems*, Offshore Technology Conference Paper Number OTC 1505, 1971.

Eames, M.C., *Approximation of Cable Configuration in Three Dimensions*, NRE Technical Note FM/64/10, September 1964.

Earle, D.H., *Towed Body Behavior in Steady Turns*, NRE Technical Note FM/66/1, January 1966.

Fabula, A.G., "Dynamic Response of Towed Thermometers", *Journal of Fluid Mechanics*, Vol. 34, No. 3, 1968.

Genin, J., *Towed Vehicle Systems*, Purdue University School of Aeronautics and Astronautics and Engineering Science, Report 66-7, July, 1966.

Genin, J., "Equilibrium Configurations and Tensions of a Flexible Cable in a Uniform Flow Field, *Journal of Aircraft*, Vol. 4, 1967.

Goeller, J.E. and Laura, P.A., *Analytic and Experimental Study of the Dynamic Response of Cable Systems*, Report 70-3, Institute of Ocean Science and Engineering, The Catholic University of America, 1970.

Jeffrey, N.E., *Analog and Digital Computer Simulation of Cable-Towed Body Systems*, NRE Technical Note FM/66/6, December 1966.

Jeffrey, N.E., Swyer, W.T. and Rozee, J.M., *Analog Computer Simulation of Towed Body Lateral-Directional Anti-symmetric Motion. Part I. Constant Coefficient Linear Equations*, NRE Technical Note FM/65/18, October 1965.

Lampietti, F.J., *Pendulation of Pipes and Cables in Water*, ASME Paper Number 63-WA-101, 1963.

Maryniak, J., *Simplified Longitudinal Stability Analysis for a Glider in Towed Flight*, NASA, U. S. Clearing House Order #N68-30263, 1968.

Mihoff, C.M., *Configuration of a Cable Towing a Submerged Body*, NRE Technical Note Math/66/1, March 1966.

Paul, B. and Soler, A.I., *Analysis of Cable Dynamics and Optimum Towing Stratigies for Tethered Submersibles*, Towne School of Univ. of Penn. Report, September 1970.

Payne, P. R., "The Terminal Forces Acting on a Light Trailing Wire", *Aero Journal of the Royal Aeronautical Society*, September 1970.

Skop, R.A., *On the Shape of a Cable Towed in a Circular Path*, Report 70-0008 in the department library, 1970.

Skop, R.A. and O'Hara, G.J., *The Analysis of Internally Redundant Structural Cable Arrays*, NRL Report 7296, 1971.

Smith, R.A., Moon, W.T. and Kao, T.W., *Experiments on the Flow About a Yawed Circular Cylinder*, Institute of Ocean Sciences and Engineering, Report 70-7, Catholic University of America, December 1970.

Tanaka, H., "Hydrodynamic and Towing Characteristics of a Modified Model of Clarke Jet Net", *Marine Biology*, Vol. 2, No. 4, 1969.

Tremills, J.A., "Feasible Depth of U/W Towed Systems, *Canadian Aeronautics and Space Journal*, Vol. 15, No. 9, 1969.

Walton, T.S. and Polachek, H., *Calculation of Non-Linear Transient Motions of Cables*, DTMB Report 1279, July 1959.

BIOGRAPHICAL NOTE

Millard Sherwood Firebaugh was born in Olney, Illinois, on May 15, 1940. He graduated from the Gilman School in Baltimore, Maryland, in June 1957. He received the Bachelor of Science degree in Physics at M.I.T. in June 1961 and was commissioned Ensign, United States Navy. He then served at sea for two years in USS MITSCHER (DL-2). In 1963, sponsored by the Navy, he returned to M.I.T. and entered the Department of Naval Architecture and Marine Engineering graduating in June 1966 with the degrees of Master of Science in Electrical Engineering and Naval Engineer. He then qualified as a U.S. Navy deep sea diver before going to the Portsmouth Naval Shipyard, Portsmouth, New Hampshire. There he worked in production as a Ship Superintendent being fortunate to participate in the construction and trials of the deep diving submarine USS DOLPHIN (AGSS-555). He re-entered M.I.T. sponsored by the Navy's doctoral study program in September 1969. Lieutenant Commander Firebaugh is a member of Tau Beta Pi and Sigma Xi. He has published an article with J.R. Melcher entitled "Traveling Wave Bulk Electroconvection Induced Across a Temperature Gradient", *Physics of Fluids*, Vol. 10, No. 6, June 1967. He is married to the former Barbara Lee McCleskey and has a son, Joshua.

Thesis
F4479 Firebaugh
An analysis of the
dynamics of towing
cables.
131522